



THE METEOROLOGICAL MAGAZINE

HER MAJESTY'S
STATIONERY
OFFICE

June 1983

Met.O. 958 No. 1331 Vol. 112

THE METEOROLOGICAL MAGAZINE

No. 1331, June 1983, Vol. 112

551.501.81:551.515.42:551.577.37(427)

Radar and rain-gauge observations of a severe thunderstorm near Manchester: 5/6 August 1981

By M. J. Bader

(Meteorological Office, Bracknell)

and C. G. Collier and F. F. Hill

(Meteorological Office Radar Research Laboratory, RSRE, Malvern)

Summary

A severe thunderstorm in the Manchester area during the night of 5/6 August 1981 produced point rainfall totals that occur, on average, less frequently than once in several hundred years at a given location. Observations of this storm from a nearby radar are used as a basis for discussion of the storm cells, the forecasts issued and how fresh insight into extreme rainfall statistics over catchment areas can be gained.

1. Introduction

Heavy, thundery rain fell over parts of England on the two rainfall days between 0900 GMT 5 August 1981 and 0900 GMT 7 August 1981. The characteristics of the rain were particularly interesting because:

- (a) the heaviest rain was concentrated in small areas only,
- (b) the amounts recorded do not occur, on average, more than once every few hundred years at a particular place,
- (c) the development of the storms was explosive and unexpected, and
- (d) the rainfall amounts and storm structure were monitored by radar, providing new insight into the validity of current guidance on rainfall for hydrological applications.

Fig. 1 shows the rainfall distribution for the two days combined. The highest totals were in three areas:

- (a) north-west England in a curved strip from Shrewsbury across the south of Manchester towards Huddersfield, with a maximum of 148 mm located 16 km east-south-east of Chester;
- (b) the south and east Midlands, with a maximum of 141 mm located west-north-west of Northampton, and
- (c) south-east England from Sussex to north-west London.

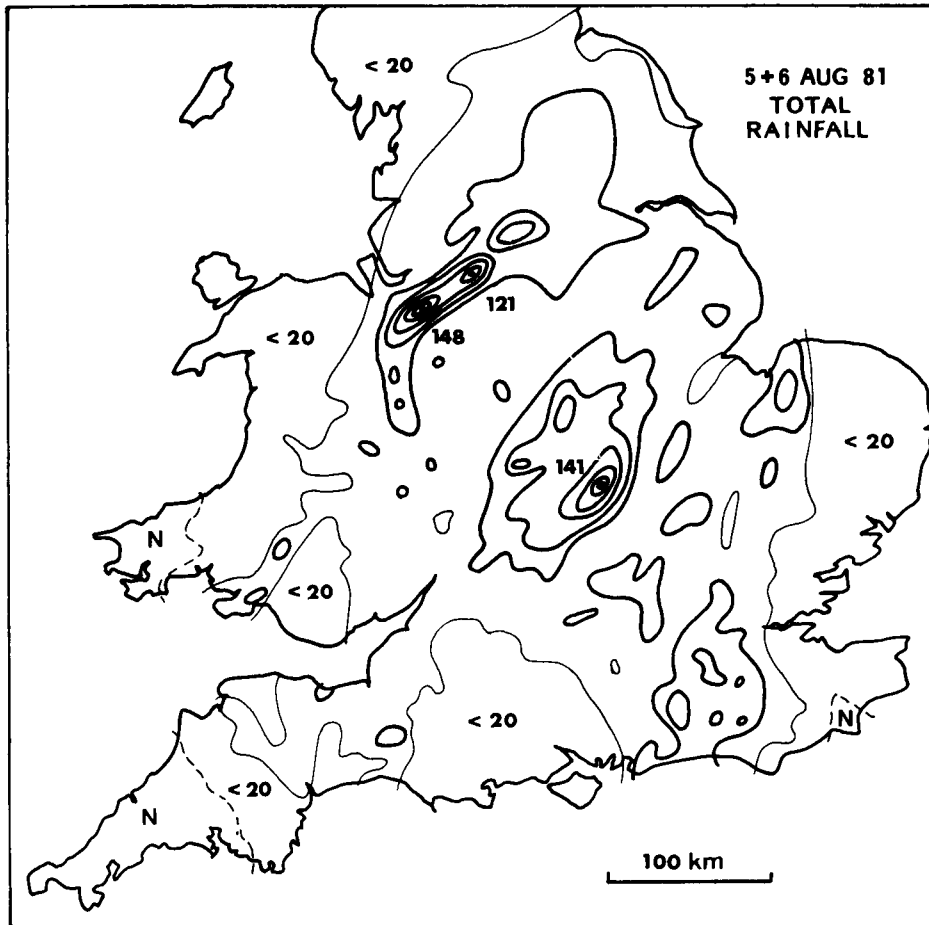


Figure 1. Total rainfall (mm) over 48 hours commencing 0900 GMT, 5 August 1981. Contours at 20 mm intervals. The thin lines are the 20 mm isohyets. (Note that there are no minima contained within any of the areas bounded by 40 mm isohyets.) N indicates areas with less than 0.5 mm.

Over north-west England most of the rain fell during the night of the 5th/6th, particularly between 2100 and 0300 GMT. The main band of storms moved across the southern part of Greater Manchester, producing serious local flooding and causing landslips (see Fig. 2). Over the Midlands, also, the heaviest localized falls occurred in the night, but here there was an additional fall of 30 to 50 mm on the 6th, most of it occurring during the daytime. Over south-east England the rain fell mostly during the morning of the 6th.

In this paper we describe the synoptic background to the thunderstorms in general before looking in more detail at the storms which produced the large totals shown in Fig. 1 over Greater Manchester. We have concentrated on this area of storms because of the proximity of the weather radar at Hameldon Hill, only 30 km to the north of the city of Manchester. This radar, which works on a wavelength of 5.6 cm and a beam width of 1° , recorded information from four different elevations every five minutes throughout the storm. Finally we discuss briefly the problem of forecasting the event.

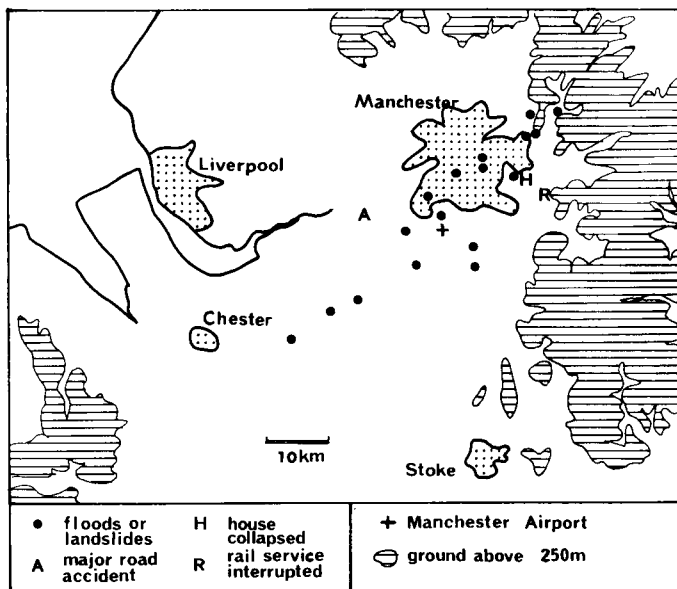


Figure 2. Location of floods and other incidents caused by heavy rain on the night of 5/6 August 1981, as collated from local newspapers.

2. Synoptic description

After a day or two of increasingly humid weather over France, the convergence associated with an intensifying upper trough caused storms to develop over a wide area and to move north-north-eastwards across England. The sequence of upper-air charts for midnight on each day from 4–7 August (Fig. 3) shows the changes that occurred at medium levels, represented by the 700 mb charts (approximately 3 km above sea level), and at high levels, represented by the 300 mb charts (approximately 9 km above sea level). At 0001 GMT on the 4th the air at medium levels was quite dry over England, moist air being evident chiefly over central France and Spain. By the early hours of the 5th an upper trough was approaching Ireland, preceded by a weak cold front, and the air at 700 mb had become moister over Biscay and western France. During the day a general backing of the airflow to a more southerly point occurred above 700 mb as the upper trough became sharper. The cold front was very weak as it crossed Ireland, giving only slight rain, and could not be easily identified at the surface.

The detailed surface analysis over the British Isles at 2100 GMT on the 5th is shown in Fig. 4. The main features are:

- (a) a slack, mainly cyclonic, north-easterly flow over England and Wales (with surface pressure rising slowly),
- (b) a tongue of hot, humid air over central England where the wet-bulb temperature exceeded 16°C, and
- (c) a cloudy region covering most of England and Wales, containing areas of unstable medium-level cloud and rain with some thunderstorms.

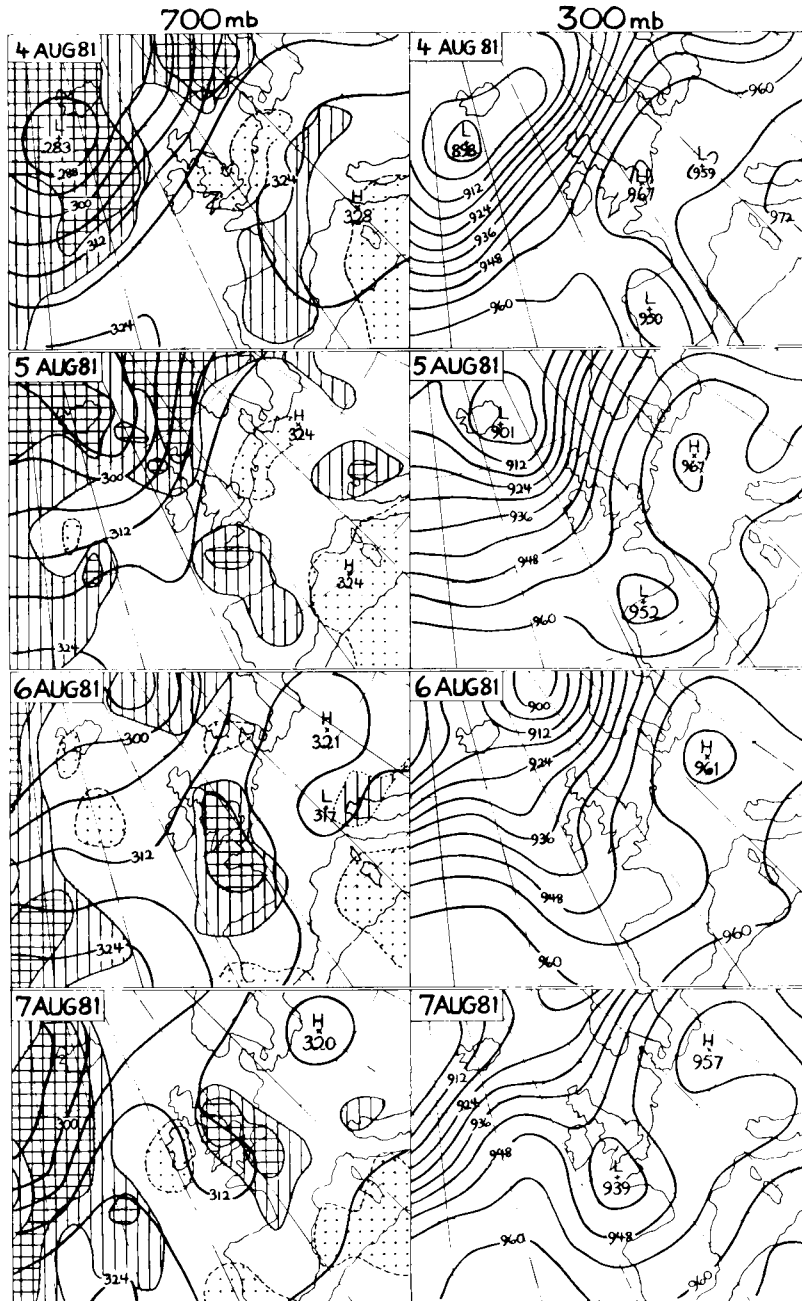


Figure 3. Upper-air analyses for 0001 GMT on 4, 5, 6 and 7 August 1981, showing the increase in relative humidity over England and north-west France at 700 mb and the formation of a sharp trough at 300 mb. Values in decageopotential metres. Relative humidity: cross-hatched $\geq 75\%$, hatched $\geq 60\%$ and dotted $\leq 30\%$.

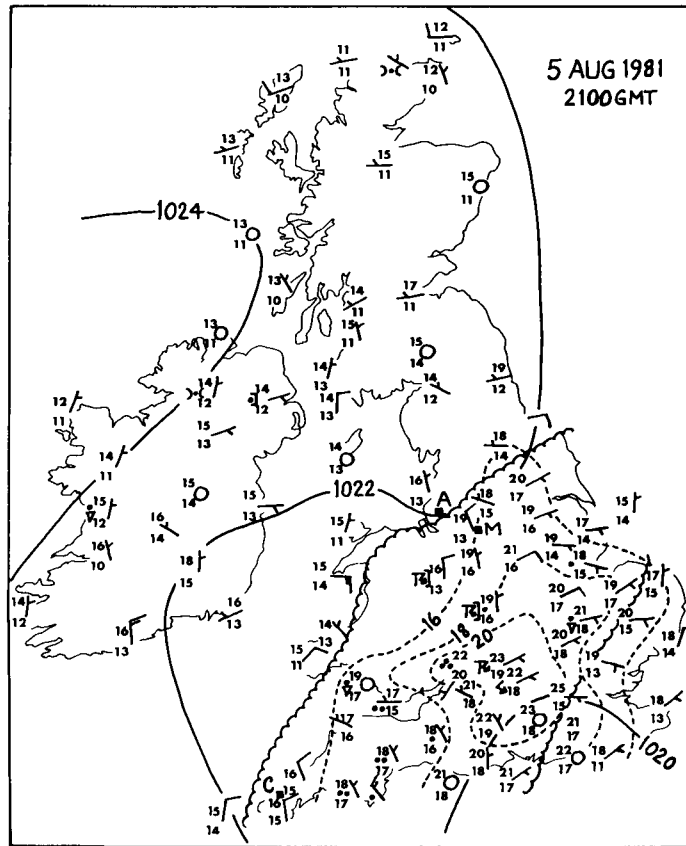


Figure 4. Surface wind, temperature, dew-point and significant weather at 2100 GMT on 5 August 1981. Continuous lines show mean-sea-level pressure (mb) and dashed lines show the region of highest wet-bulb temperature ($^{\circ}$ C). Stations in England and Wales bounded by the wavy lines reported $\geq \frac{3}{8}$ cloud. Areas of unstable medium-level cloud were present within this cloudy region. The positions of Camborne, Aughton and Manchester Airport were marked with C, A and M respectively.

The nearest radiosonde station to Manchester is Aughton (Fig. 5). Here, the air was potentially unstable from 925 to 590 mb. The air at medium levels was dry because the main cloud mass was to the south-east; the Camborne ascent, which was probably more representative of the medium-level air associated with the Manchester storm, showed moist, potentially unstable air from 750 to 500 mb. The widespread release of that potential instability was responsible for the large area of cloud and thundery rain shown in Fig. 4.

Fig. 6 shows the distribution of rain at stated times during the 5th and 6th as observed by the radar network. Areas of thundery rain moved north-eastwards to reach the south-west of England by late afternoon on the 5th, while other storms developed over east Wales and the Midlands (Fig. 6(a)). During the evening, these storms moved north-north-eastwards towards northern England. The storms over eastern Wales, however, moved on a more northerly track towards the Shrewsbury area until 2100 GMT, when they began to move in a north-easterly direction towards Manchester. During the night new areas of thundery rain moved north across the Channel Islands and Cherbourg Peninsula towards

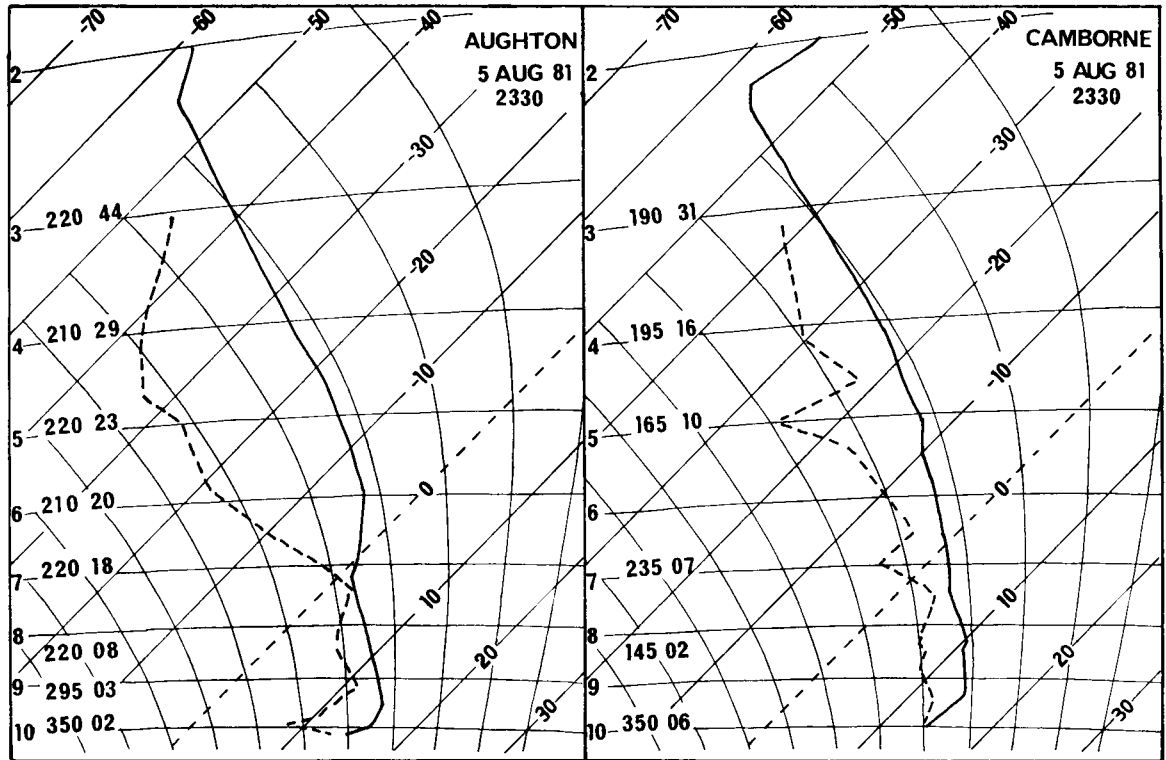


Figure 5. Tephigrams from the surface to 200 mb for Aughton and Camborne at 2330 GMT, 5 August 1981. Winds in degrees true and knots.

southern England (Figs 6(b) and (c)). These storms (Fig. 6(d)) were particularly violent over the London area around 0900 GMT. Gradually the more active storm areas moved northwards while the earlier storms died away to form large areas of persistent, but less intense, rain over the Midlands and northern England (Figs 6(e) and (f)). Drier weather extended north-eastwards across most of England during the night of the 6th/7th, but the upper trough was slow to clear the country and pockets of rain persisted over some northern parts throughout the 7th.

3. Rainfall over north-west England on 5–6 August 1981

3.1 Analysis of the rain-gauge data

Fig. 7 shows the rainfall totals over north-west England for the 24 hours ending 0900 GMT on the 6th. Two characteristics of the rainfall pattern are worthy of note:

- (a) the banded nature of the area of heavy rain, and
- (b) the small areas covered by the heaviest rainfall.

The strip of heaviest rain consisted of five main maximum fall areas (see also Fig. 1); two were orientated south/north near Shrewsbury and the other three were aligned south-west/north-east

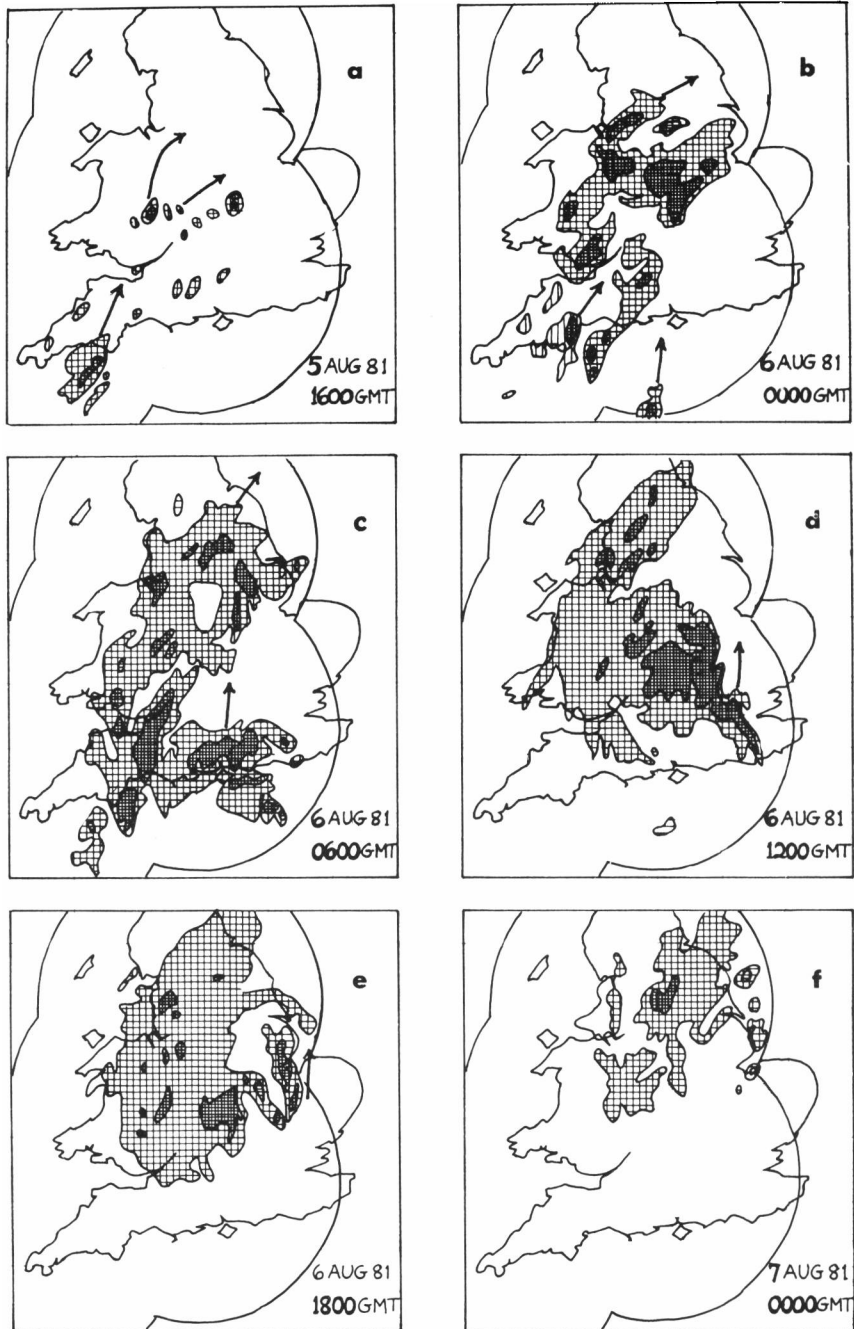


Figure 6. The cross-hatching (coarse and fine) depicts areas of rain shown by the radar network, effective within the circular boundaries. Fine cross-hatching shows rainfall rates exceeding approximately 4 mm h⁻¹. Arrows indicate movement during the interval from the current frame to the next frame, where this was not obscured by decay or new development.

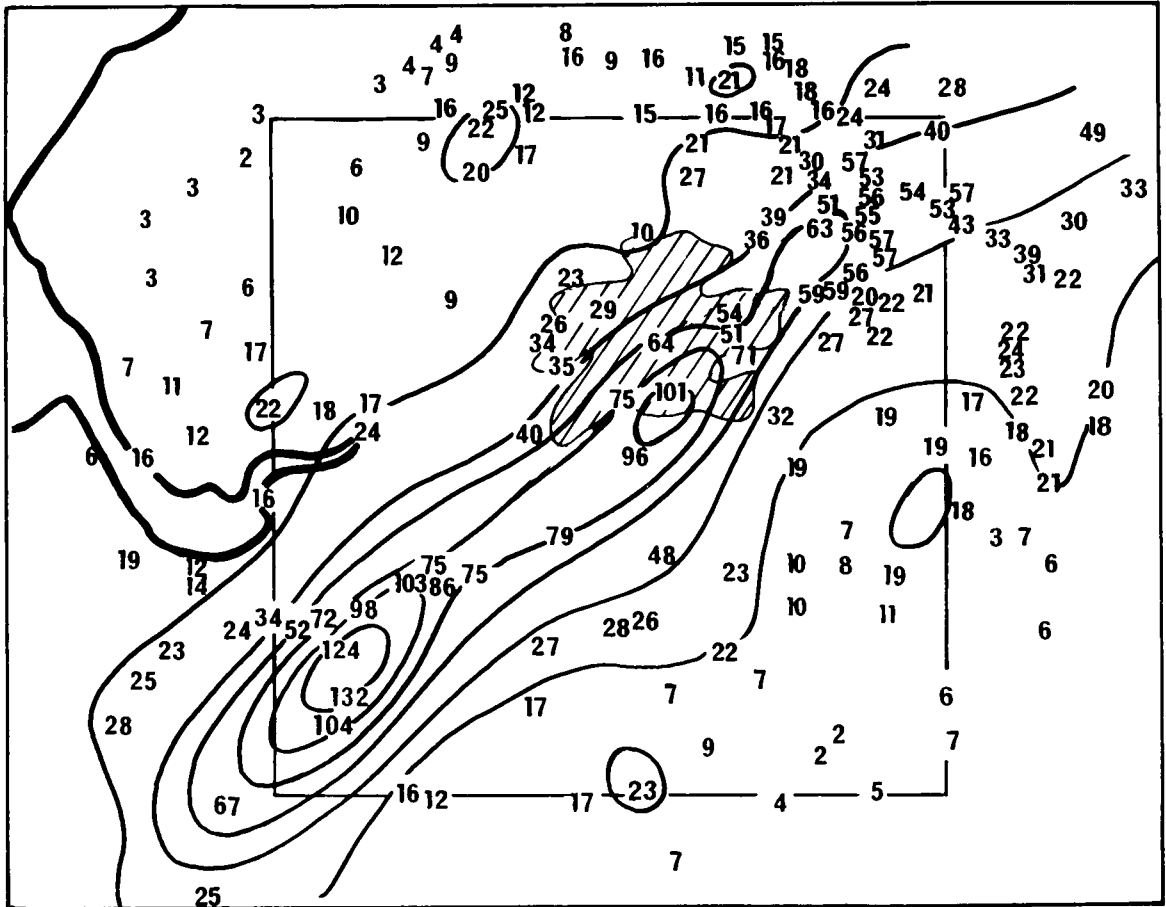


Figure 7. Rain-gauge totals (mm) for 24 hours commencing 0900 GMT, 5 August 1981. Contours at 20 mm intervals. Hatched area indicates Greater Manchester. The square locates the radar area used in Fig. 9. The totals of 101 and 96 mm were recorded at East Didsbury and Manchester Airport respectively. The highest total, 132 mm, occurred at Eaton Pumping Station.

towards the Pennines. The highest total of 132 mm was recorded at Eaton Pumping Station, 16 km east-south-east of Chester, but there were no data available from recording gauges in this area for resolving the rainfall for a duration of less than one day. However, the centre of the next maximum was situated to the south of Manchester where recording gauges were sited.

At Manchester Airport, most of the rain fell between 2200 GMT on the 5th and 0300 GMT on the 6th. The rainfall trace from the airport is shown in Fig. 8(a); the intense rain after 0100 GMT is well shown. The rainfall total for the five-hour event beginning at 2218 GMT was 89.8 mm. This corresponds to a return period of nearly 800 years. The characteristics of the rainfall at the airport were fairly typical of the rainfall in the surrounding area. However, East Didsbury, 7 km north-east of the airport, was nearer the centre of the maximum rainfall (Fig. 7); here, 85.3 mm of rain fell in 2 hours 40 minutes (Fig. 8(b)). This value corresponds to a return period of a little over 1000 years. Although the rainfall amounts from the Manchester storm were rare, much higher point totals have been recorded for similar durations; for example, 169 mm fell in 2½ hours at Hampstead, London, in 1975 (Keers and Wescott 1976).

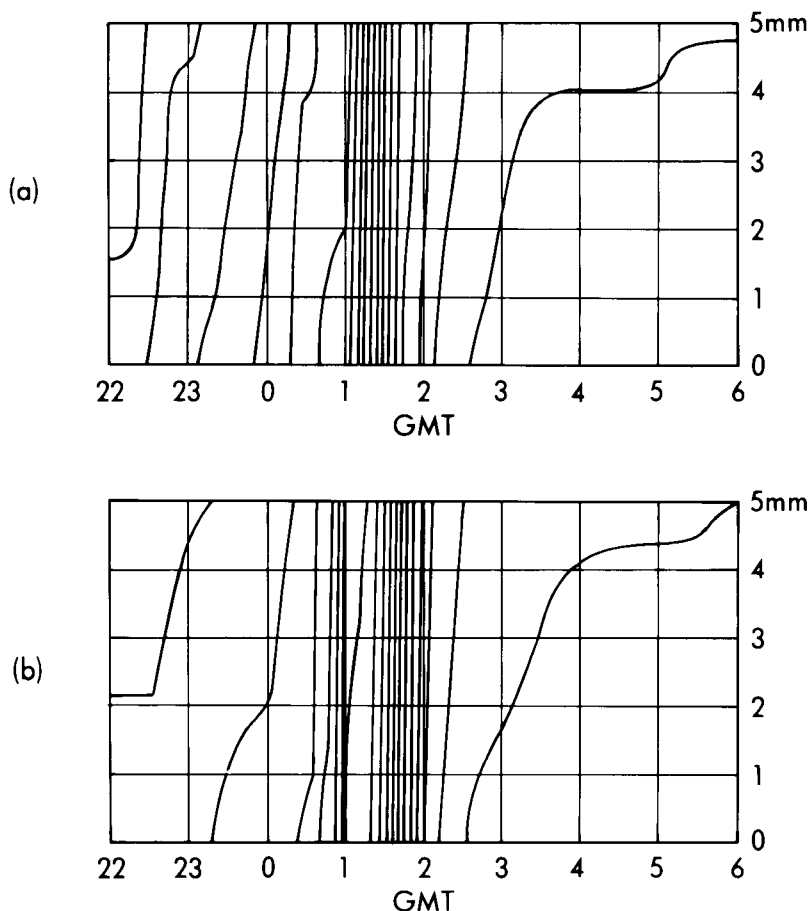


Figure 8. A copy of the rainfall trace at
 (a) Manchester (Ringway) Airport,
 (b) East Didsbury (Parrs Wood).
 The stations are about 7 km apart and are situated within the same maximum rainfall area (see Fig. 7). The abscissa is time, in hours GMT; the ordinate is rainfall in mm. One full-scale deflection corresponds to 5 mm.

3.2 Radar observation of the storms

This description of the storms is based on the radar data collected at Hameldon Hill from all four elevation scans (0.5° , 1.5° , 2.5° , 4°). Because of ground clutter, which affects the lowest beam in a north/south direction immediately to the west of Manchester, the shape and intensity of the storms are indicated more reliably by the 1.5° scan. In order to eliminate any large errors in the rainfall rates derived from the radar data (using the standard relationship $Z = 200R^{1.6}$, where Z is the radar reflectivity factor ($\text{mm}^6 \text{m}^{-3}$) and R is the rainfall rate (mm h^{-1})), a comparison was made between the five-minute radar data, integrated throughout the whole period of the storm, and the total rainfall measured around 0900 GMT. The ratio of radar to rain-gauge totals was mostly between 1.0 and 1.5 in the vicinity of the main rain-band. An overestimate is to be expected since Z will exceed $200R^{1.6}$ whenever the precipitation contains large water drops or hail (Battan 1973) and can be influenced by strong vertical air motions (Battan 1976). Some small areas of much higher ratios occurred to the south of the storms; these are

believed to have been caused by anomalous propagation (Battan 1973). In the following description of the progress of the storms, illustrated by Fig. 9, the rainfall intensities associated with cells A, B, C and D have been obtained by dividing the radar data by 1.0, 1.3, 1.1 and 1.4 respectively, while anomalous echoes have been eliminated.

Fig. 9 shows the position of the storms at 20-minute intervals across a 60×60 km square centred near Manchester Airport. The band of rain approximately 60 km long and 40 km wide was orientated in a north-east/south-west direction. The principal storm centres occurred on the south-eastern side of the band, producing steep rainfall gradients on this side, whereas an area of gradually diminishing rainfall rate extended over a 30 km range to the north-west of the storms. The general east-north-east progression of the envelope of rain belies the complexity of developments within it. Progression appears to have been caused by the development of new cells at about 40-minute intervals to the north-east of existing storms. Thus the cell labelled A in Fig. 9 remained some 40 km south-west of Manchester for about two hours, giving the heaviest rain (about 80 mm h^{-1}) around midnight. At this time the rain area appeared to split, with cell B moving east-north-east for a while to reach Manchester Airport by 0100 GMT while cell A drifted very slowly eastwards and weakened. Cell B became slow-moving near the airport and another cell, C, intensified some 20 km to the north-east. These cells in combination gave a 20 to 25 km long swathe of heavy rain exceeding 60 mm h^{-1} from 0100 to 0140 GMT. Cell D formed around 0100 GMT to the north-east of cell C and became the main centre by 0200, although it probably did not give rain heavier than 60 mm h^{-1} . Both cells B and C weakened quickly after 0145 GMT and cannot be identified as separate entities by 0210 GMT.

Comparison of Figs 7 and 9 shows that the three rainfall maxima in the daily totals coincide with the positions in which cells A, B and D were almost stationary.

4. Estimates of the areal rainfall associated with the Manchester storm

Hydrologists are particularly interested in rainfall amounts over areas, and radar has the potential for meeting this requirement. The snapshots provided by the radar at five-minute intervals were therefore used as a basis for calculating the highest amounts of rain that fell over areas consisting of one 5×5 km square, four squares (100 km^2) and nine squares (225 km^2). These were 99, 81 and 72 mm, respectively, in $2\frac{1}{2}$ hours. The corresponding totals for the Hampstead storm, which produced one of the highest point totals ever recorded in the United Kingdom, were 104, 56 and 35 mm (from Keers and Wescott 1976). Thus over 25 km^2 the totals from the two storms were similar, but over larger areas the rainfall from the Manchester storm was heavier. Remembering that the point rainfall from the Hampstead storm was much greater (section 3), it may be concluded that point rainfall from gauges whose spacing is comparable with or greater than the scale of rainfall variability can be a misleading indicator of areal storm rainfall. However, radar-derived data have the potential for providing more realistic values of catchment area rainfall, provided of course that the adjustment factors can be calculated accurately.

Similar considerations apply to hydrological design for which rainfall amount-area-frequency relationships derived from climatological records are used. To take the extreme case, in the design of hydrological structures that must have a high safety factor, the concept of Probable Maximum Precipitation (PMP) is used. This is the highest amount of rain that is likely to fall over the area and for the period appropriate to the catchment in question. According to the *Flood Studies Report* (Natural Environment Research Council 1975), the two-hour PMP for Manchester over 25, 100 and 225 km^2 areas is 143, 132 and 127 mm respectively. In the *Flood Studies Report*, PMP for this duration is used as a reference for computing PMP for other durations, so it is an important quantity to calculate correctly.

It is expected that PMP over a catchment on the ground would be produced from storm cells, like those in the Manchester storm, that remained quasi-stationary during their most intense phase. The

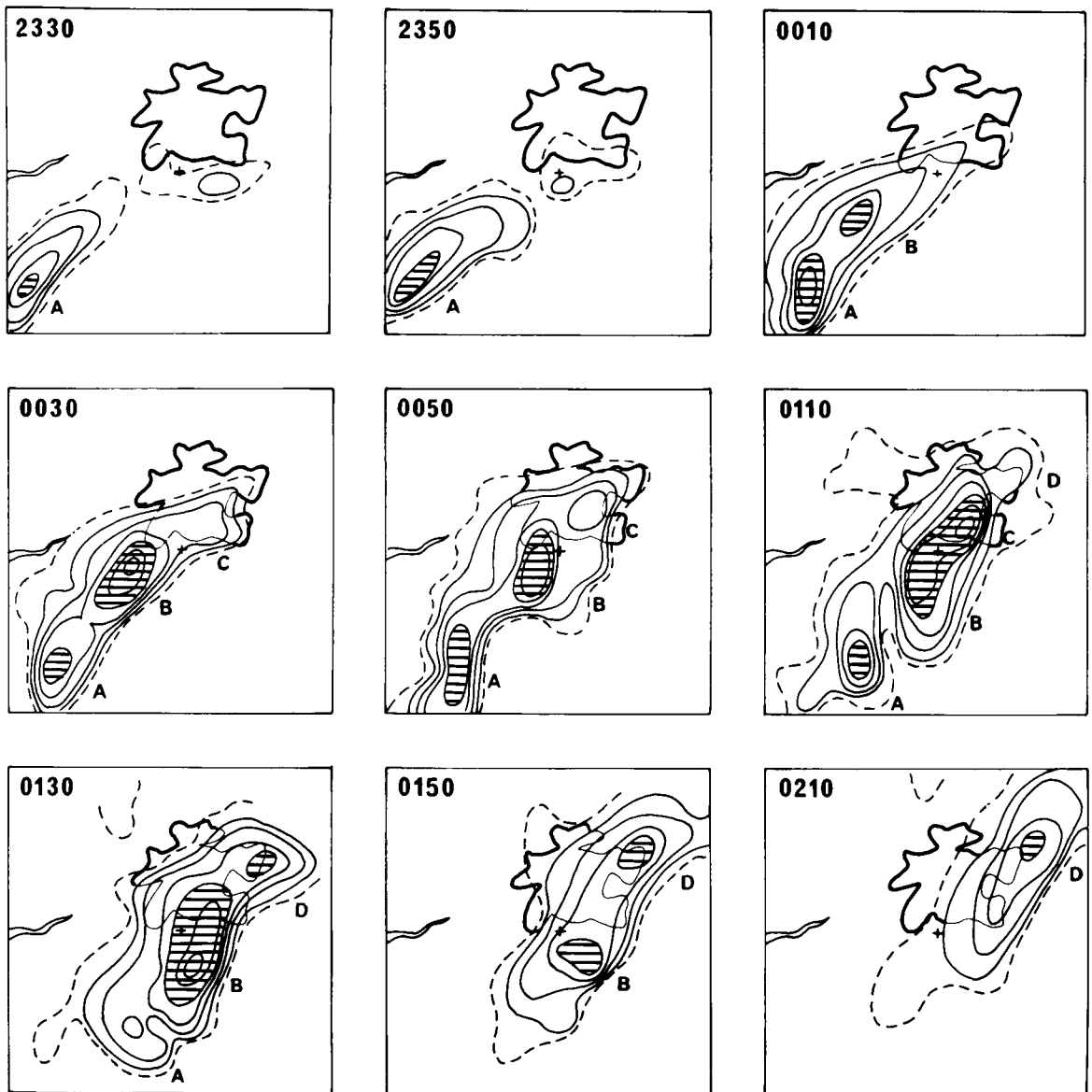


Figure 9. Progress of storms across a 60×60 km square centred near Manchester Airport (indicated by +). Contours are drawn at 5 mm h^{-1} (dashes), then multiples of 10 mm h^{-1} , with intensities over 40 mm h^{-1} shown by hatching. Letters identify individual storm cells. Solid outline shows the boundary of Greater Manchester. The radar is located at Hameldon Hill, which is 44 km north of Manchester Airport.

significance of the figures in the *Flood Studies Report* can therefore be assessed by using the radar data to calculate the rainfall from a cell as it moves along, i.e. in the Lagrangian frame of reference. The two-hourly totals for cell B (Fig. 9) were 145, 114 and 86 mm over 25, 100 and 225 km² respectively. Thus over 25 km² the observed total is similar in magnitude to the *Flood Studies Report* value of PMP.

During the hour when cell B was most active (0045 to 0145 GMT), the rainfall total over 25 km² of 83 mm was similar to that from other recent storms (Table I) that were studied using radar data. Thus, while it may be argued that the rainfall statistics over a particular catchment area are determined by the distribution of cell velocities as well as the rain that falls from the cells, the rainfall amount from cells like cell B may occur quite often and a larger sample of storms than that shown in Table I may reveal an even higher areal rainfall. Indeed, it is reasonable to envisage, given a favourable wind structure, two cells like cell B within a multi-cellular storm that deposit their rain over the same catchment area during their most intense phases. If so the *Flood Studies Report* PMP over 25 km² would be exceeded. Similar comparisons (see Table I) reveal that the *Flood Studies Report* PMP over 100 km² could be reached. Over 225 km², however, the PMP would not be reached, even though cell B produced much higher rainfall than the other storms studied — a fact that, given a larger sample, may add to the rarity of the Manchester storm.

Table I. Hourly areal rainfall (mm) from storm cells in the Lagrangian frame of reference.

Date	Location	Rainfall area		
		25 km ²	100 km ²	225 km ²
5 June 80	Darwen, Lancs.	60	37	24
20 May 81	East Pennines	83	51	30
1 June 81	Bournemouth	68	41	29
9 July 81	Derby	76	46	32
6 August 81	Manchester	83	66	51

The analysis of the Manchester storm shows how radar can broaden our knowledge of areal rainfall. Provided the radar data can be calibrated accurately, using 'ground truth' from gauges (as on this occasion), the data have potential for providing new insight into the catchment rainfall climatology, widely used for hydrological design.

5. Forecasting

The north-eastward movement and intensification of storms on 5 August were not well forecast. On the 4th a continuation of the dry weather was anticipated over most parts of England and Wales for the 5th and 6th. Though a risk of isolated thundery activity was recognized, associated with the vortex present on the 4th (see Fig. 3) moving north-eastwards across Biscay and northern France and weakening, this activity was expected to affect only south-east England and the Channel Isles. Early forecasts during the night of the 4th/5th told a similar story but when the Malvern radar network display in the Central Forecasting Office (CFO) at the Bracknell Meteorological Office showed echoes approaching the south-west around dawn on the 5th, a special synoptic review extended the risk area into much of southern England and South Wales. More widespread outbreaks of thundery rain were still only expected in the south-east following numerical guidance based on 0001 GMT data on the 5th which showed precipitation bounded by a line south-west/north-east through The Wash.

By the afternoon of the 5th, CFO were forecasting activity south-east of a line from the Severn to the Humber. Rectangle 10-level model forecasts based on 1200 GMT data gave good guidance with some large totals expected in the north-west Midlands overnight but unfortunately the output was four hours late arriving in CFO. By this time outbreaks were already occurring over Wales and these were being followed on radar.

The main reason for the thundery activity being more widespread than originally predicted was the failure to handle the complex evolution of the upper trough involving the north-eastward relaxation of the vortex over Biscay (Fig. 3), the disruption of the fast-moving Atlantic trough (positioned to the west of Ireland at 0001 GMT on the 6th) and the subsequent sharpening of its disrupted southern portion as contour heights rose rapidly upstream. The extension of this feature into Biscay considerably altered the flow pattern over the United Kingdom by the 6th and contributed to the widespread precipitation on that day, which was subsequently well forecast, but it appears to have occurred too late to contribute to the weather events over the United Kingdom on the 5th. The critical inflow of very moist, warm air at medium levels during the 5th appears to have been the result of a northward movement of a forward part of the Biscay vortex (as shown by the spread of medium-level cloud into south-west England and Wales) rather than north-eastward as predicted.

Although the broad-scale guidance from CFO did not provide an accurate forecast many hours in advance of this event, the availability of the real time Malvern radar composite displays in both CFO and at Manchester Airport did allow the development of the storms to be monitored closely. Using radar data at 15-minute intervals the local forecaster at Manchester Airport was able to modify the forecast for his area, in conjunction with CFO, as soon as it became evident that the radar was showing an extension of the storm development northwards. This led to the issue of a thunderstorm warning for Manchester Airport at 1937 GMT on the 5th. An alert was also passed to the duty hydrologist of the Mersey and Weaver Division of the North West Water Authority at 1955 GMT. By 2040 GMT Manchester Air Traffic Control had been briefed about the storms and warnings were then issued to aircraft, particularly light aircraft.

To have provided a more detailed forecast would have required foreknowledge that the storms which were over Shropshire at 2000 GMT would persist for several hours and veer to a more north-easterly track. Persistence is not always a reliable predictor since analysis of the radar data shows much variation in the duration of rainfall within storms. With regard to their movement, it is clear that winds above 600 mb had a stronger westerly component at Aughton than at Camborne (Fig. 5), though even at Aughton winds remained backed with respect to the general east-north-eastward displacement of the storm cells. Perhaps the stronger westerly components in the north contributed to the change of track observed after 2100 GMT. Such detail cannot be provided by current observational networks or operational numerical models with grid lengths of 50 kilometres or more, but may be provided eventually by remote sensing techniques and the development of numerical models with grid lengths of a few kilometres.

6. Conclusion

On the night of 5/6 August 1981, serious damage was caused in the Manchester region as a result of intense rain. Point rainfall amounts measured near Manchester during the storm occur on average only every few hundred years and, in this sense, the event can be described as rare. The banded distribution of heaviest rain at the ground as shown by the gauge observations can be explained by the north-eastward transfer of the main storm, as revealed by observations from the radar at Hameldon Hill. The radar analysis also provided new insight into areal rainfall amounts: the similarity in magnitude between the areal rainfall from this storm and the areal 'Probable Maximum Precipitation' in the *Flood Studies*

Report throws new light upon the current guidance given for engineering design purposes and further careful radar-based analysis of storms is needed.

Local forecasts of the event provided several hours warning of the thunderstorms over Manchester, but were unable to define the intensity of the rain which actually resulted. At present, radar and geostationary satellite imagery offer the only prospect of detecting the areas of development and for providing warnings with some lead time, even though this might be rather short on occasions. We hope that it will be possible in the future to use operational numerical models with a grid length of a few kilometres to forecast the preferred areas of development and rainfall amounts from storms caused by motions on the mesoscale.

Acknowledgements

The Hameldon Hill radar data were collected as part of the North West Radar Project which was jointly set up by the Meteorological Office, the North West Water Authority, the Water Research Centre, the Central Water Planning Unit and the Ministry of Agriculture, Fisheries and Food. We also acknowledge the kind provision of thermograph and anemograph data by Keele University. Thanks are also due to the Principal Meteorological Officer, Manchester Airport, and the Deputy Assistant Director (Central Forecasting) who provided details of the forecasts actually issued.

References

- | | | |
|--------------------------------------|------|--|
| Battan, L. J. | 1973 | Radar observations of the atmosphere. The University of Chicago Press. |
| | 1976 | Vertical air motions and the Z-R relation. <i>J Appl Meteorol</i> , 15 , 1120–1121. |
| Keers, J. F. and Wescott, P. | 1976 | The Hampstead storm — 14 August 1975. <i>Weather</i> , 31 , 2–10. |
| Natural Environment Research Council | 1975 | Flood Studies Report. Vol. II, London. |

Regional-scale interannual variability of climate — a north-west European perspective

By C. K. Folland

(Meteorological Office, Bracknell)

Summary

Climatic variability on space scales ranging from 10^7 km² (mainly North Atlantic and north-west Europe) to local areas (10 km²) within the United Kingdom (UK) is discussed with emphasis on relations between the characteristics of variability in space and time. A comprehensive study of monthly, seasonal or interannual variability has scarcely commenced so the bulk of our digested knowledge exists mainly on local and regional space scales. Even here, analyses have been dictated often more by practical than theoretical considerations, so our understanding of the causes of variability is, not surprisingly, meagre.

1. Introduction

The current state of knowledge about short period variability has progressed quite modestly since Craddock (1964) wrote: 'Research work concerned with the slower changes in the atmosphere is at the stage typified by Kepler rather than Newton in that its main task is that of assembling facts and recognising regularities and patterns rather than seeking explanations'.

Perhaps as (1981) emphasized by Hastenrath and Kaczmarczyk '... the characteristic time scales of climate and circulation variability, and the preferred frequency bands for spatial coherence [of such variability] have received little attention'.

2. Structure of the subject

Many empirical studies have been made of short period (a month to a few years) climatic fluctuations but the results are difficult to assess and to integrate. No unifying theory exists of regional interannual climatic variability or climatic variability from month to month, except to a limited extent that of the seasonal cycle. The analytical procedures vary greatly, geographical scope is usually limited and the purposes of analyses often reflect sharply-defined practical requirements. It is, above all, difficult at present to gain an appreciation of the spatial characteristics of time sequences of short period fluctuations. This reflects the difficulty of designing appropriate analyses though some use has been made of time series analysis in studies of longer term fluctuations.

Most studies could be grouped as follows (some combine several forms of analysis):

- (a) Case studies of individual 'events'.
- (b) Multiple case studies: 'superposed epoch analysis', 'analogue selection' in long-range forecasting (LRF), 'multivariate analysis'.
- (c) Time series studies.
- (d) Studies of the frequency or probability of 'events'.
- (e) Studies of associations of one type of data with another (correlation and regression).
- (f) Eigenvector analysis.

Analyses of types (e) and (f) will not be discussed in detail here, but Nicholls (1980), for example, gives a review of some applications to LRF.

3. What is the problem?

We need to explain or predict variations or 'spells' of weather like those illustrated below.

Example 1 — January 1963 (Figs 1(a) and 1(b))

January 1963 was persistently 'blocked' and very cold, as was much of the three months December to February, with a surface high north of Scotland. Winds were therefore mainly easterly over UK. The Iceland Low essentially disappeared and the jet stream was split between a branch south and another north of the block. The winter of 1962/63 was the coldest since 1739/40 in some places and blocking was generally more evident than usual over the Northern Hemisphere (Murray 1966, Namias 1963). (See also section 5.2.)

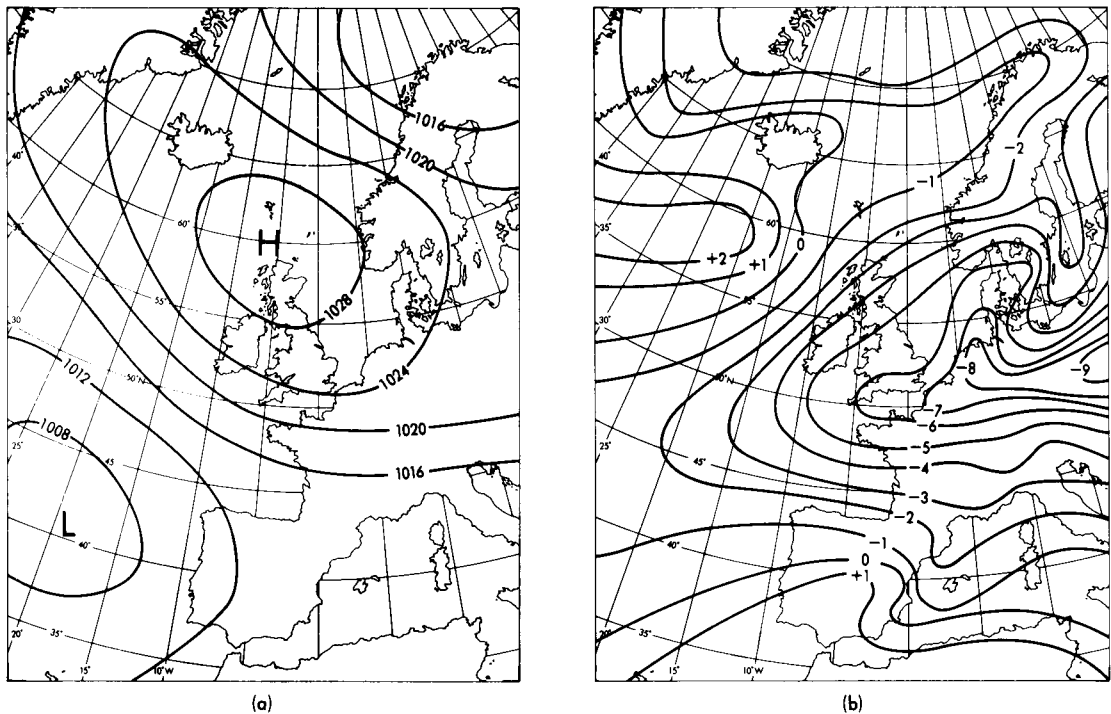


Figure 1. (a) Average pressure (mb) at mean sea level, January 1963.
(b) Average screen-level temperature anomaly (°C), January 1963. (Anomalies mainly from 1931–60 station averages.)

Example 2 — January 1974 (Figs 2(a) and 2(b))

January 1974 was stormy; the Iceland Low was exceptionally deep and persistent. This mild and westerly month in north-west Europe was an extreme example in the 'spell' of four such winters from 1971/72 to 1974/75 (Wright 1975, Painting 1976).

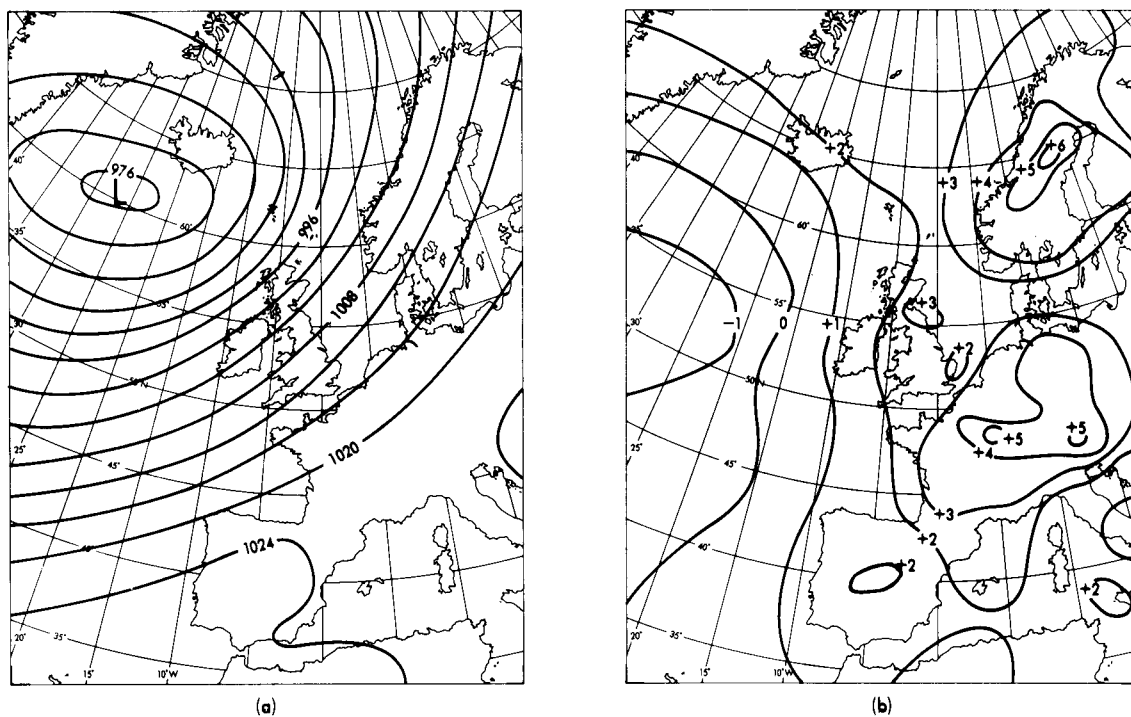


Figure 2. (a) Average pressure (mb) at mean sea level, January 1974.
 (b) Average screen-level temperature anomaly (°C), January 1974. (Anomalies mainly from 1931–60 station averages.)

Example 3 — summer and autumn 1976 (Figs 3 and 4)

Summer 1976 was exceptionally dry and warm; the jet stream was persistently far to the north-west or north of the UK (Fig. 3), and frequently anticyclonically curved in UK longitudes. Consequently summer 1976 was one of the warmest in the last 300 years in parts of England, and exceptionally dry (Ratcliffe 1977, Miles 1977 and Murray 1977).

The transition to Autumn in 1976 was startlingly abrupt and in some ways contrary to the normal seasonal changes. The jet stream, from early September, became positioned persistently over, or south of, southern England (Fig. 4). Thus depressions frequently passed over, or were quasi-stationary near, southern England, (the jet stream tends to stay near northern Scotland in September). Autumn 1976 was the second wettest in many southern areas since at least 1727. (See also section 5.1.)

Example 4 — May 1975–August 1976 (Fig. 5)

Summer 1976 was the culmination of an even more exceptional ‘spell’. The conditions shown in Fig. 3 were maintained with only short breaks (though the jet stream was generally slightly further south) during May 1975–August 1976 (Ratcliffe 1977, Miles 1977). Consequently May 1975 to August 1976 was the driest 16-month period in England and Wales (EW) since at least 1727. A Minister for Drought was appointed as the water supply dwindled and other consequences of the drought became severe (Folland 1978 gives summary). Fig. 5 shows the mean-sea-level pressure pattern and its anomalies over the



Figure 3. Average positions of mid-troposphere jet streams and their directions of flow for most five-day periods in summer 1976.

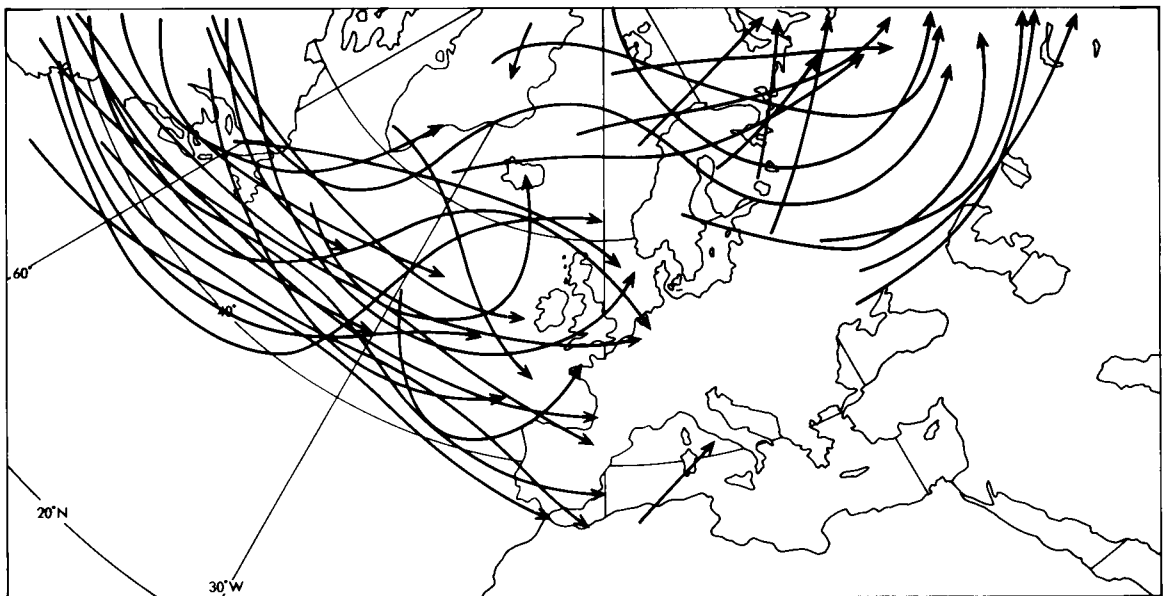


Figure 4. Average positions of mid-troposphere jet streams and their directions of flow for most five-day periods in autumn 1976.

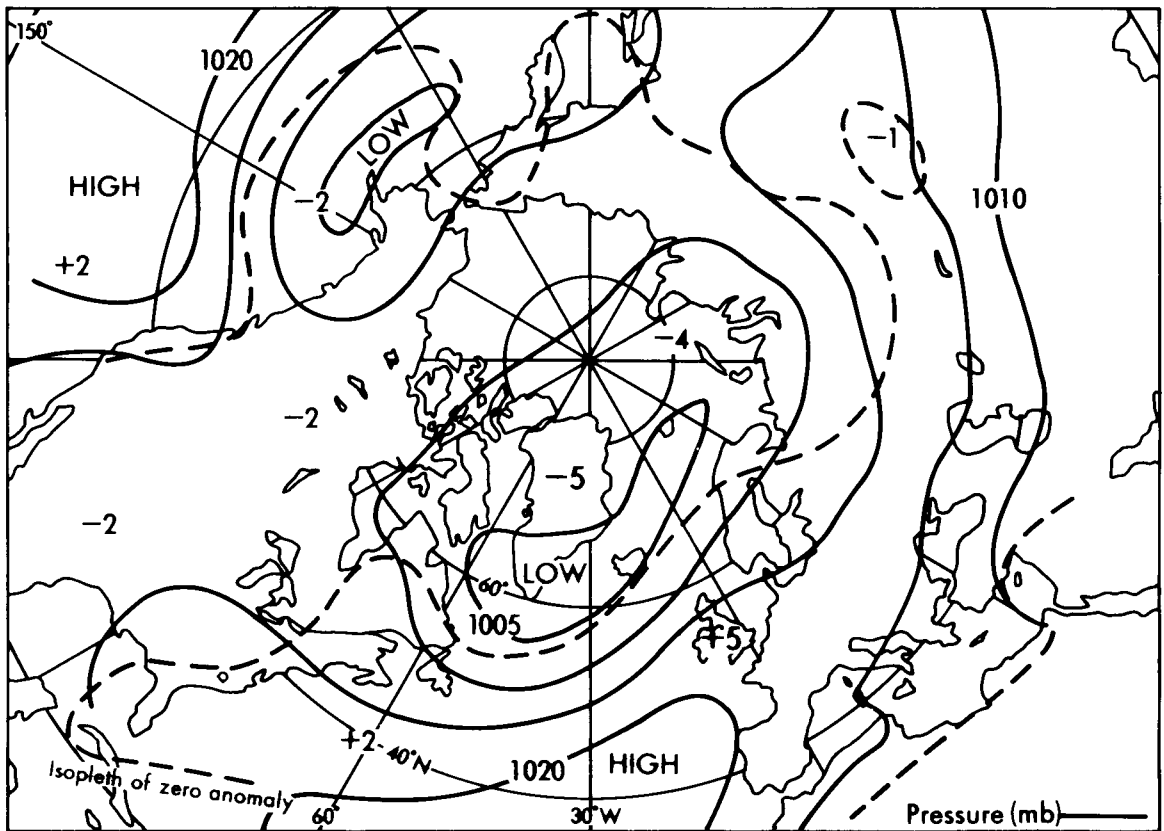


Figure 5. Average pressure (mb) at mean sea level and its most prominent anomalies from 1951-70 average, May 1975-August 1976.

period; the positive and negative anomalies near England and Greenland respectively are both exceptional being about three standard deviations (3σ) from average. The 500 mb geopotential anomalies were similarly placed so that, curiously, 1000-500 mb thicknesses were generally near average (see also section 5.1). Other exceptionally long 'spells' affecting the UK include the 1921 drought and the 1878-80 cold spell, both of surprising persistence and intensity.

A general discussion of long 'spells' is given in Lamb (1972).

4. A problem of interpretation

Many problems can arise in interpreting the unusualness or extent of weather anomalies from climatic data*. The variability of weather elements is difficult to define uniquely, as variabilities in time and space are intimately related. The problems mainly arise because variations at one point do not have the same amplitude or even phase, if sufficiently distant, as those at other points (Rodriguez-Iturbe and Mejia 1974 give a mathematical discussion for rainfall). Figs 6 and 7 give examples of the variation of the

*The word 'anomaly' is used in this paper to describe deviations of weather elements from their average at a given time of the year; the paper is mainly concerned with North Atlantic and north-west European area anomalies.

correlation coefficient (r) with distance, Fig. 6 for monthly summer rainfall at Kew with monthly summer rainfall at other points over EW and Fig. 7 in graphical form for temperatures averaged over about 2.2, 3.4 and 5 years between a number of stations distributed over Europe, adapted from Schönwiese (1979). Note the difference of space scale between the two examples for a given value of r ; monthly rainfall in summer over EW is much more poorly correlated at a given distance than is temperature over Europe when averaged over a few years. These diagrams also reflect the fact that the statistical structure of anomalies at points differs considerably from that over large areas. For example the $\pm 3\sigma$ anomalies in Fig. 5, which may each be expected to occur about once every 300 years on average (described as a 'return period' of 300 years), invite the question — climatic change? The perspective alters when it is realised that a $\pm 3\sigma$ point anomaly of surface pressure average over a year, for example, is likely to occur somewhere almost every year (Miles 1977).

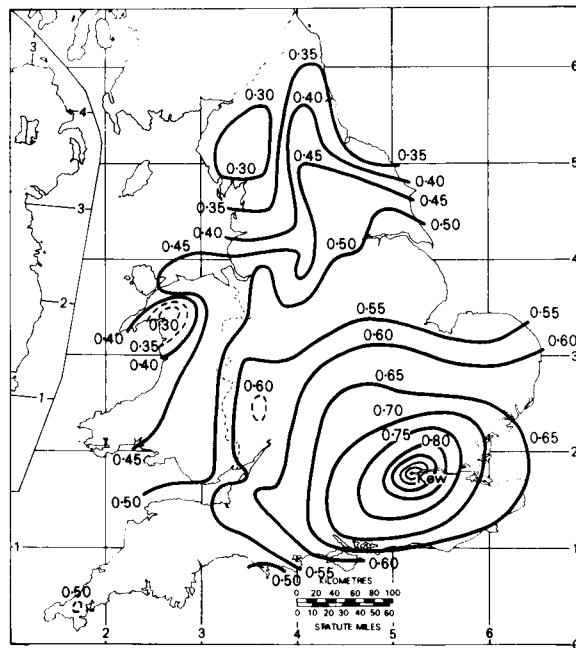


Figure 6. Correlation coefficient of monthly rainfall with that at Kew; summers 1911-70. Mean of June, July and August.

5. Two case studies

5.1 1975-76 drought (May 1975-August 1976, introduced in sections 3 and 4)

Fig. 8(a) shows that the 1975-76 drought covered much of western Europe (Fig. 8(a) actually covers October 1975-July 1976). Ratcliffe (1977) and Ratcliffe and Morris (1976) noted that the 500 mb mean jet stream near the UK appeared to move fairly steadily northwards between summer 1974 and summer 1976 (Fig. 8(b)). They considered that the northward movement may have been aided by a steady northwards and westwards recession (at a given season) of sea ice near east Greenland (Fig. 8(b)) that commenced after 1969. The recession was thought to be related to unusually stormy conditions in that region during the 'westerly' winters of 1971/72 to 1974/75 (mentioned in section 3). They suggested that the jet stream would tend to be moved northwards and westwards with the ice edge as a result of the

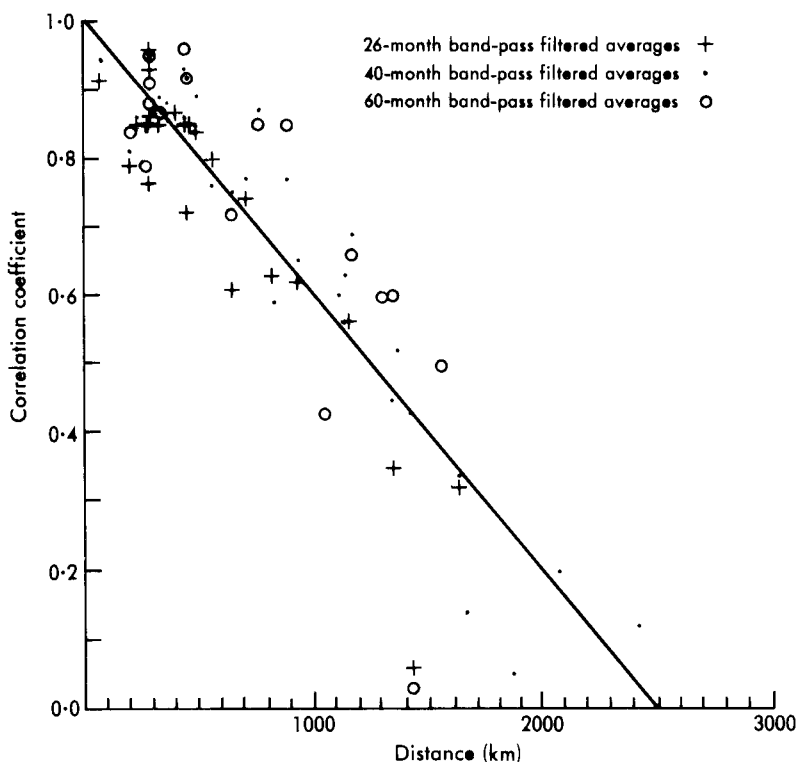


Figure 7. Inter-correlation of station temperatures measured in Europe for three averaging periods: 26 months, 40 months and 5 years.

accompanying movement of the strong (near surface) thermal gradient. Also noted was a sharp decline in Pacific sea surface temperatures (SST) north of 40°N and west of 150°E relative to those temperatures further south in most months from late 1974 to late 1976. The 1000–500 mb thickness gradient in mid-Pacific near 45°N was enhanced (at least in association) and 500 mb mid-Pacific zonal flow averaged 20% above normal during the drought period. Northern Hemisphere summers with noticeably strengthened 500 mb flow and those with weakened flow in this region were compared; on average the former were considerably drier and more anticyclonic over England and Wales. Similar effects were noted in winter; a study of the historical records indicated that anticyclonic tendencies were also strengthened in the presence of a stronger than normal east Canadian trough, as was observed in winter 1975/76. The generally westerly phase of the stratospheric quasi-biennial oscillation during the drought, at least until spring 1976, was also considered important in helping to maintain the east Atlantic jet stream in a northerly position (Parker 1982). Other factors were also considered (see Ratcliffe 1977). By summer 1976 some of the postulated influencing factors were waning or had disappeared; the persistence and great heat of the drought in the summer of 1976 was ascribed to anomalously efficient conversion of solar radiation to sensible heat as little evaporation would occur over the dry ground, so maintaining a strong local thermal ridge over western Europe. Finally at the end of the summer, with a decline in local solar heating, it was thought that the now altered hemispherical influencing factors forced a sudden change in the position of the jet southwards, so the drought ended very abruptly. These associations or ‘teleconnections’ have yet to be confirmed.

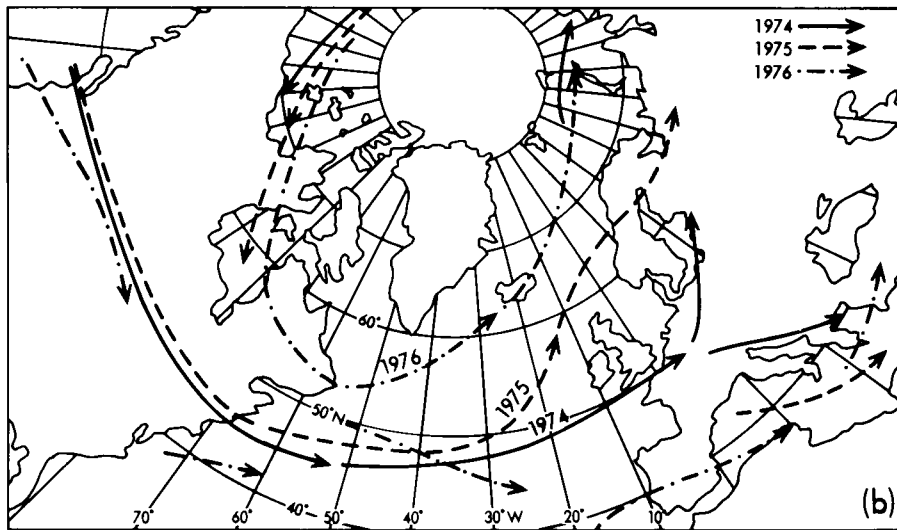
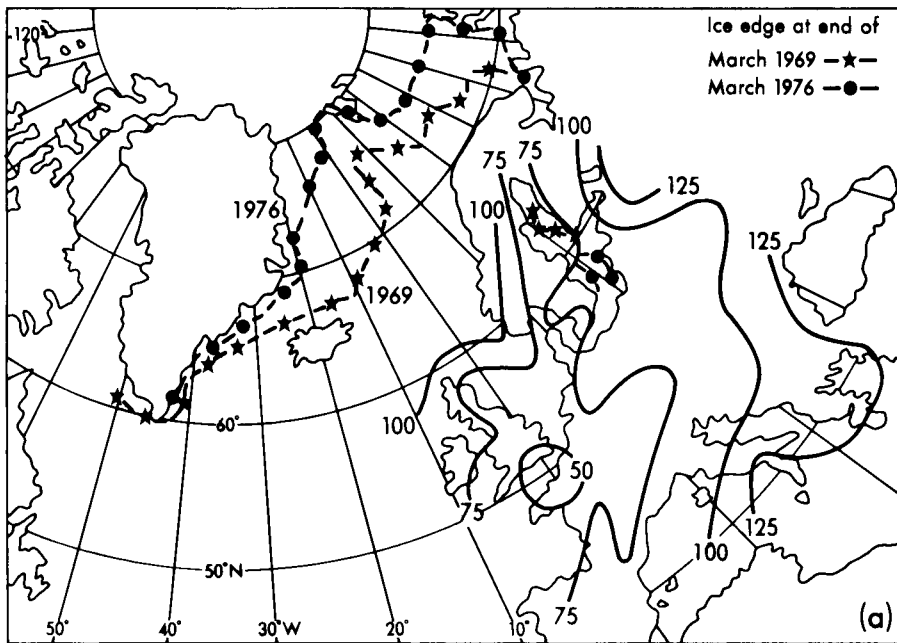


Figure 8. (a) Rainfall expressed as percentage of long term average in Europe, October 1975–July 1976, and position of ice edge March 1969 and March 1976. (After Ratcliffe and Morris 1976).

(b) The average position of the jet stream in the middle troposphere in July and August in the successive years 1974–76.

A similar, briefer, drought occurred in the period from August to November 1978 (Bader and Warrilow 1979). This drought also ended abruptly and was followed by a wet, cold winter with the jet stream again returning to a southerly position. Fig. 9 shows the positions of jet streams during autumn 1978, the size of the positive surface pressure anomaly and the area it covered, and the extent of the drought. The return period of the rainfall deficiency (average expected time, deduced from past records,

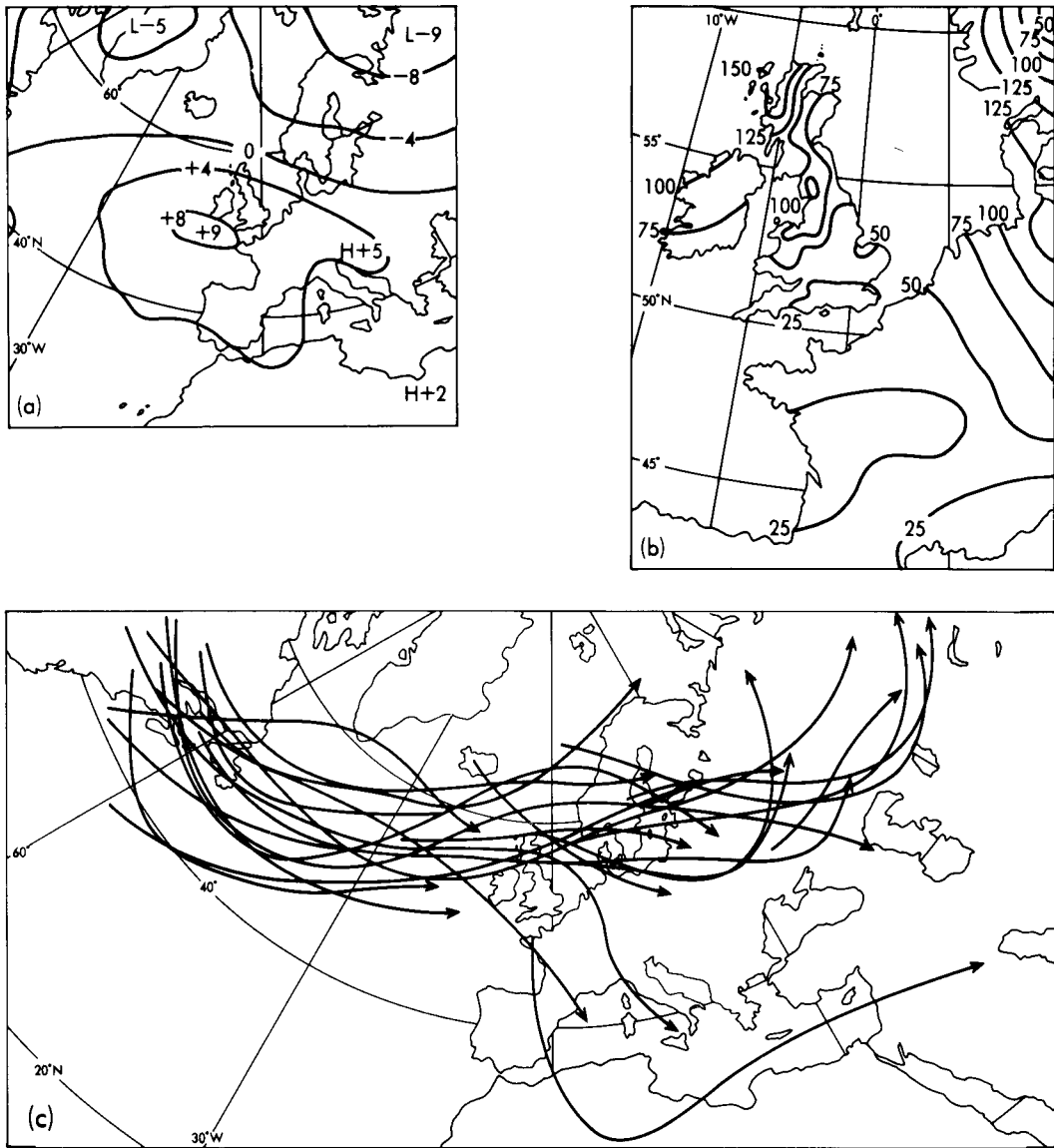


Figure 9. (a) Average pressure anomaly (mb) at mean sea level, September–November 1978. (Anomalies from 1951–70 averages.) (b) Total rainfall, expressed as a percentage of average September–November 1978. (Averaging period mainly 1931–60.) (c) Average positions of mid-troposphere jet streams and their directions of flow for most five-day periods in September–November 1978.

between rainfall deficiencies as or more severe than that under study) and its severe effect on the volume of two reservoirs in south-west England is shown in Fig. 10. This quite severe drought caused much concern to water engineers as it occurred so soon after the apparently very rare 1975–76 drought.

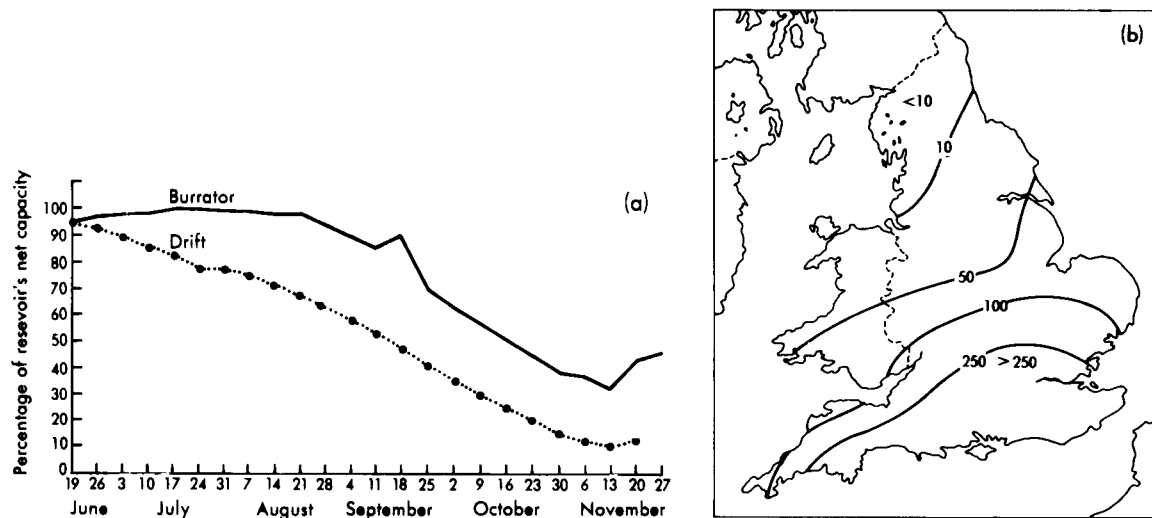


Figure 10. (a) The change in the volume of water in two reservoirs in south-west England, June–November 1978, measured as a percentage of the reservoir capacities.

(b) Autumn 1978 rainfall return periods (years) for England and Wales.

5.2 1962/63 winter: a case study involving the test of a hypothesis

Following on from previous work and, for example, the general ideas of Sawyer (1965), Rowntree (1976(b)) tested a hypothesis that widespread anomalously warm SST in the tropical North Atlantic helped to maintain the blocked, cold 1962/63 winter over the UK. Work using general circulation models had suggested that warm SST in the tropical North Pacific affected the winter-time mid-latitude Pacific atmospheric circulation (Rowntree 1972). Furthermore, in idealized numerical experiments on 'tropical forcing' Rowntree (1976(a)) confirmed the general possibility of such mid-latitude circulation effects, for example as a result of anomalous warmth or coldness in the tropical oceans, though significant forcing may be confined largely to the winter half-year. At this time of year the mid-latitude westerly circulation at upper levels often reaches as far south as latitude 15°N , above the trade winds. Rowntree noted that a wide expanse of the North Atlantic ocean surface waters between West Africa and South America was over 1°C above average in January 1963 (area marked on Figs 11(a), (b) and (c)) with a maximum anomaly of 2.8°C close to the West African coast near 17°N . These anomalies had mostly formed in Autumn 1962, before the winter circulation developed. The results of three pairs of experiments with and without the anomaly are shown in Figs 11(a), (b) and (c). Experiment 1 started from an isothermal atmosphere while experiments 2 and 3 started from real data, 29 December 1965, and differ only in model details. The results differ markedly, though experiments 2 and 3, especially, are in broad agreement. All experiment pairs show a maximum fall of pressure centred about 40° (experiment 1) or 25° (experiments 2 and 3) north of the anomaly. Experiments 2 and 3 show marked pressure rises near $60\text{--}70^{\circ}\text{N}$. In experiments 2 and 3, an easterly wind anomaly is evident near 60°N extending southwards over England though the observed anomalies implied by Fig. 1(a) are larger.

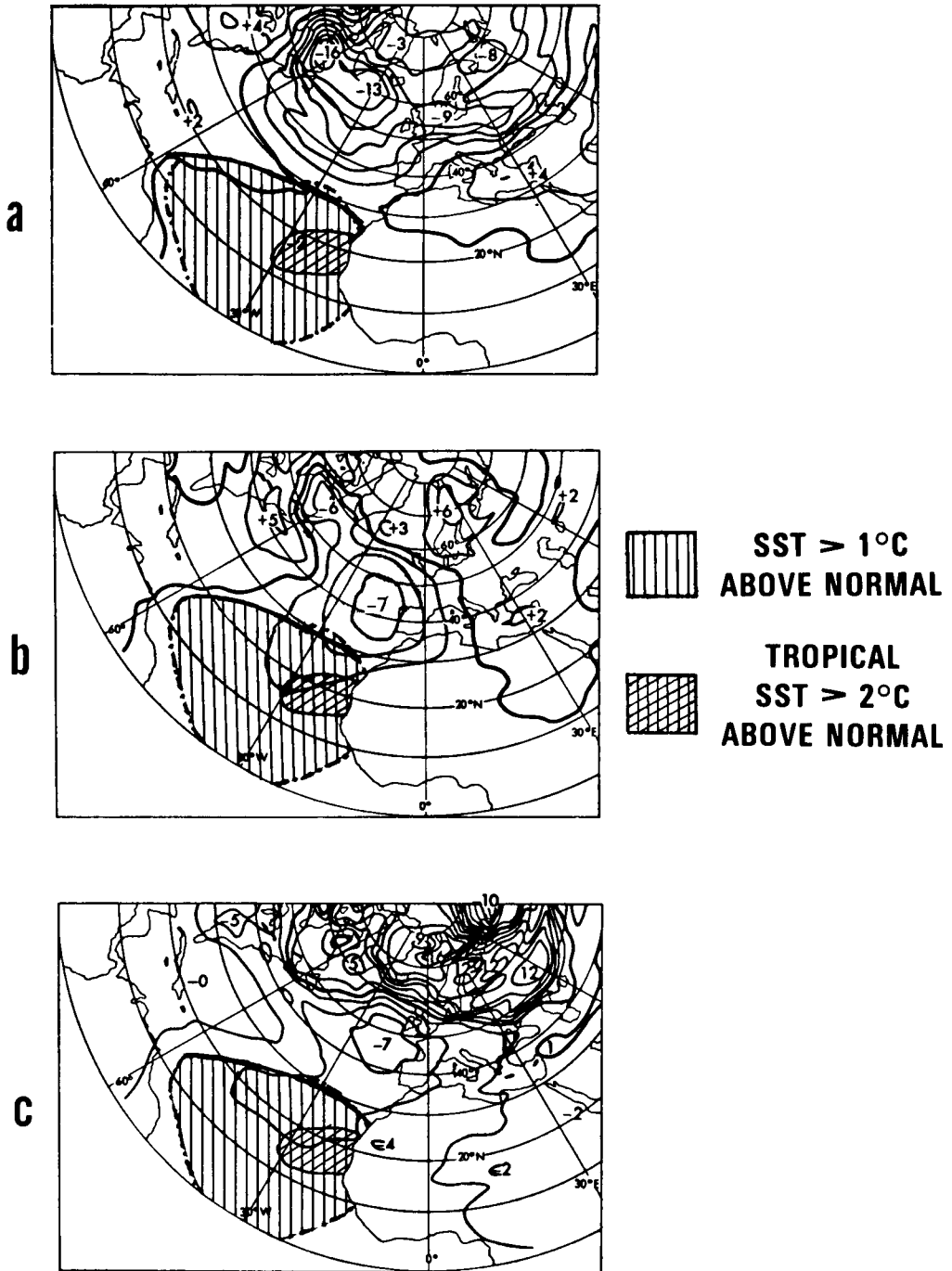


Figure 11. Difference in mean surface pressure (mb) averaged over days 41–80 of model integrations between surface pressure obtained with tropical Atlantic warming and the control experiment without the warming. (a) experiment 1 using isothermal initial data, (b) experiment 2 using initial real data, and (c) experiment 3 also using initial real data. Both (b) and (c) use initial data for 29 December 1965. SST averages taken from US Naval Oceanographic Office data.

The fall of pressure well north of the SST anomaly and the rise further north still could be regarded as manifestations of a forced standing wave in the meridional direction; model results (and the real data) showed that this wave-like effect extended high into the troposphere. Observed surface pressure data for the ten winters associated with the highest air temperatures at Mindelo, Cape Verde Islands (17°N, 25°W) and the ten winters with the lowest air temperature at Mindelo in the period from 1921–22 to 1969–70 were compared to the mean for the same period. Winter air temperature and sea temperature at Mindelo were thought to be well-correlated so the coldest winters at Mindelo should correspond to the coldest SST values and warmest winters to the warmest SST values. The average of the warm SST years gives a pressure anomaly pattern consistent with that of the 1962/63 winter though the pattern is much weaker (Fig. 12(a)). The average of the cold years gives an almost exactly reversed pattern in the North Atlantic (Fig. 12(b)), though it is again weak. This case study indicates the promise of the complementary use of modelling and observational studies, even though the results require further confirmation.

6. Superimposed chart analysis (SCA) and superposed epoch analysis (SEA)

SCA (sometimes called composite chart analysis) is illustrated by Rowntree's construction, discussed above, of two surface pressure anomaly charts each representing the average of winters selected according to their SST at Mindelo. In general SCA involves identifying and averaging one or more classes of fields of a variable selected according to their association with 'key' conditions. Differences between, and the consistency of, the data making up the composite charts can be studied. A related method is known as superposed epoch analysis, terminology usually reserved for analyses of recurrence tendencies in time series. Terms of the time series are classified according to the time elapsed since the occurrence of a key condition which recurs through the time series. The terms in each class are then averaged. The dates of the key conditions are called 'key dates'. Hypotheses are sometimes directly generated by the results of SEA or SCA. In Rowntree's analysis on the other hand SCA was used to support an independently arrived at hypothesis. However, in another well-known analysis by Ratcliffe and Murray (1970) SCA was essentially used to generate an 'a posteriori' hypothesis. Values of monthly mean-sea-level pressure over the North Atlantic and western Europe associated with monthly mean SST in an area near Newfoundland in the previous month were calculated and the result used to provide a long-range forecasting tool. The key conditions were the sign of the SST anomaly and the name of the calendar month of the year, giving a total of 24 SCA patterns. Difficulties can arise both with the assessment of the statistical reality of such results and with the objective selection of key conditions. Korevaar (1982) discusses, critically, difficulties encountered with objectively identifying SST patterns for use as key conditions in a subsequent extension by Ratcliffe of this work. Haurwitz and Brier (1981) provide a balanced critical discussion of the use of SEA, concentrating on a specific example of its use. Nevertheless, SEA and SCA can be valuable methods of exploratory analysis, well-illustrated together in a recent study by Rasmusson and Carpenter (1982) of variations in atmospheric wind circulation associated with different phases of the Southern Oscillation.

7. Time-series analysis

The full range of available time series techniques has perhaps hardly been used in meteorology. Meteorological time series are typically 'noisy'; nevertheless, a simple plot of the data against time is often useful and may be revealing. Fig. 13 shows a time series providing unexpected information. The largest 2-hour duration rainfalls (Jenkinson 1975, p. 31) recorded in each year (these would all be convective storms) were calculated for 22 stations in south-east England for a 20-year period, the 22

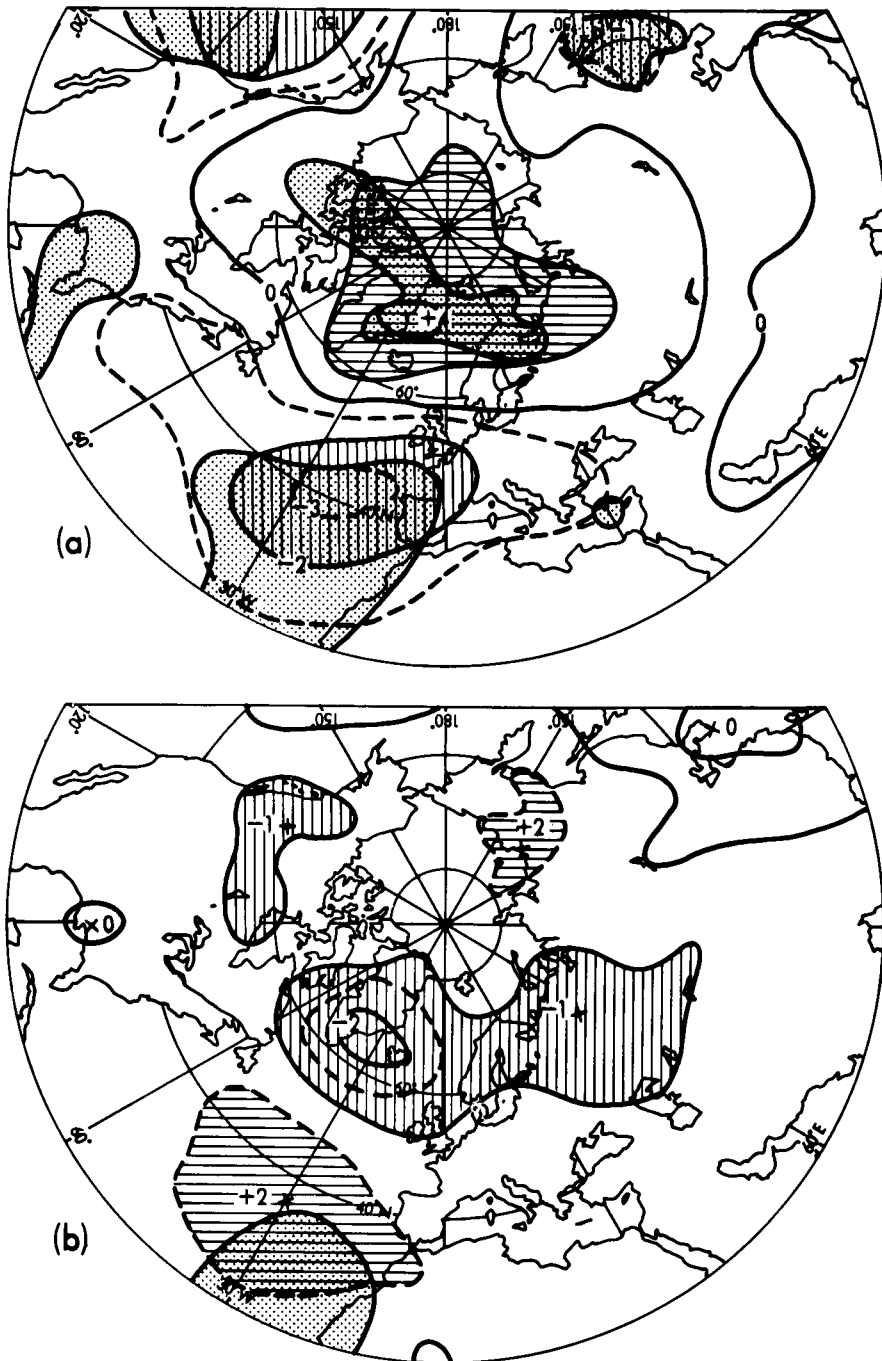


Figure 12. Average winter (December–February) pressure anomalies (mb) at mean sea level relative to 1921–22 to 1969–70 for (a) ten winters with highest air temperatures (b) ten winters with lowest air temperatures at Mindelo, Cape Verde Islands. Areas significant at 5% confidence level (Welch test) are stippled.

values observed in a given year were averaged and the averages plotted as a percentage of their median value as shown in Fig. 13. The time series is surprisingly well correlated from one year to the next for such an apparently transient phenomenon. Rainfalls of this type are of especial practical interest to urban drainage design engineers. (See section 8.2.)

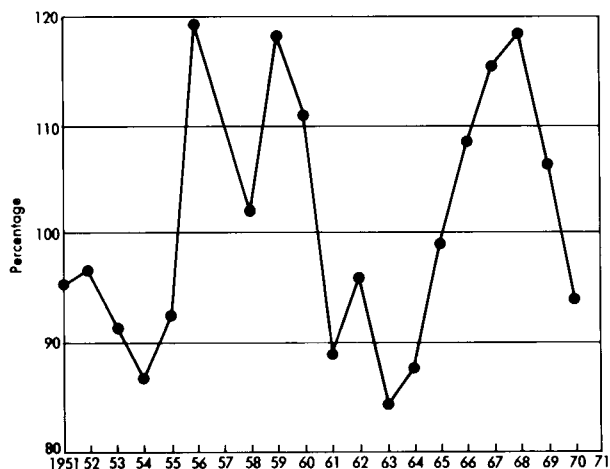


Figure 13. Two-hour annual maximum rainfall as a percentage of its median value for 22 stations in south-east England over a 20-year period.

More complex analyses are often needed. Power-spectrum analysis is one type where variation of a data series in time, for example the series of annual Central England Temperature (CET) 1659–1980 based on Manley (1974), is converted to variations of the data according to their frequency or wavelength. Cyclical or 'quasi-cyclical' recurrences can be identified; Fig. 14 shows a power spectrum of annual CET (Mason 1976). Wavelength near 2.1–2.4 years, 23 years and 90 years are particularly prominent. Such spectra can however be misleading; annual CET spectra calculated for independent, shorter periods show substantial variations. Filtering analysis is a way of studying the variations of data of a particular wavelength (frequency) range through time. Fig. 15 shows a study of the '23-year' wavelength filtered series of annual CET, where variations at and near this wavelength have been isolated. The amplitude of the series has varied greatly although the progressive decline with time of its amplitude may not indicate purely 'random' behaviour. Also shown is the lack of consistency of phase between these CET fluctuations and the 'Hale' or double-sunspot cycle often associated with climatic variability on this wavelength.

Many other forms of time-series analysis are used in meteorology, for example, the system mainly due to Box and Jenkins. See Gray (1976) for references and an application of these techniques.

It may be more valuable to study the time variation of whole fields of variables. A pioneering study was that of Sawyer (1970) who investigated the time variation of Northern Hemisphere 500 mb, 1000–500 mb thickness and surface pressure fields using filters. He contrasted the spatial behaviour of these parameters on synoptic or near synoptic time-scales (generally less than 15 days) and 'long-range forecast' time-scales (about 20–60 days). He found the ratio of the root-mean-square (r.m.s) 500 mb geopotential on the 20-day to 60-day time-scale to that on the synoptic and near synoptic time-scales was surprisingly large in some areas and spatially very variable, though Sawyer's investigation was limited to

a few years of data. Fig. 16 shows the results for the period 1961–63, where all seasons have been analysed together. A high ratio of r.m.s. variation on the 20-day to 60-day time-scale to that on the shorter time-scale is noticeable near UK. He also found a generally higher correlation between 500 mb geopotential, 1000–500 mb thickness and surface pressure anomalies on the 20-day to 60-day time-scale than the synoptic and near synoptic time-scales. Recently other workers have extended these analyses and show, for example, very high correlations between 500 mb geopotential variations and surface pressure variations over the north-east Pacific and north-east Atlantic on time-scales of about one month (e.g. Blackmon et al. 1979).

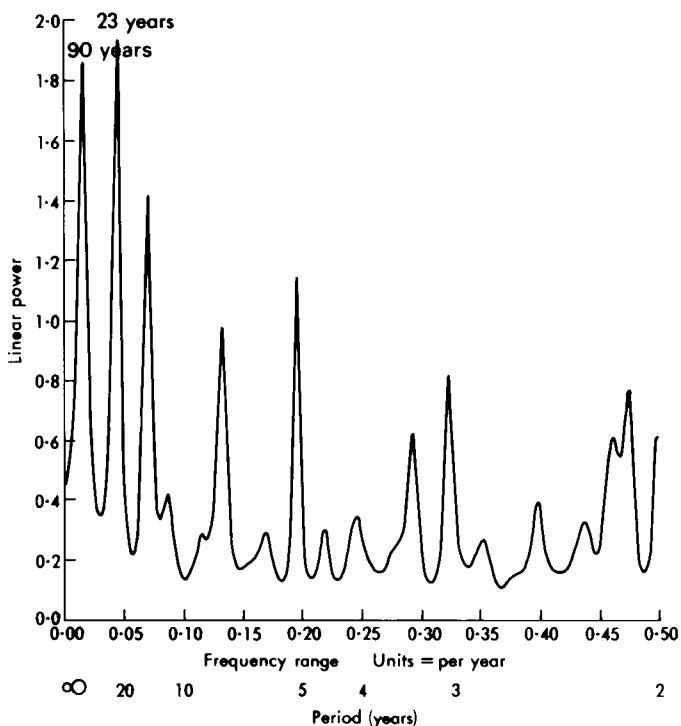


Figure 14. Maximum entropy power spectrum of Central England Temperature 1659–1974.

8. Practical application of studies of the probability or frequency of climatic events

Much of the application of climatic data to engineering and agricultural problems has involved this type of analysis. The numerical values from past data of a climatic variable are ranked and the return periods of the values, especially very large or very small values, are assessed for planning purposes.

8.1 Long duration rainfall — droughts and prolonged wet spells

Tabony (1977) provides a very detailed statistical model and computer programs (available in the Meteorological Office) for estimating the return periods of rainfall amounts in any one month up to any five-year period for any place or area in the United Kingdom. Fig. 17 illustrates a typical result from the

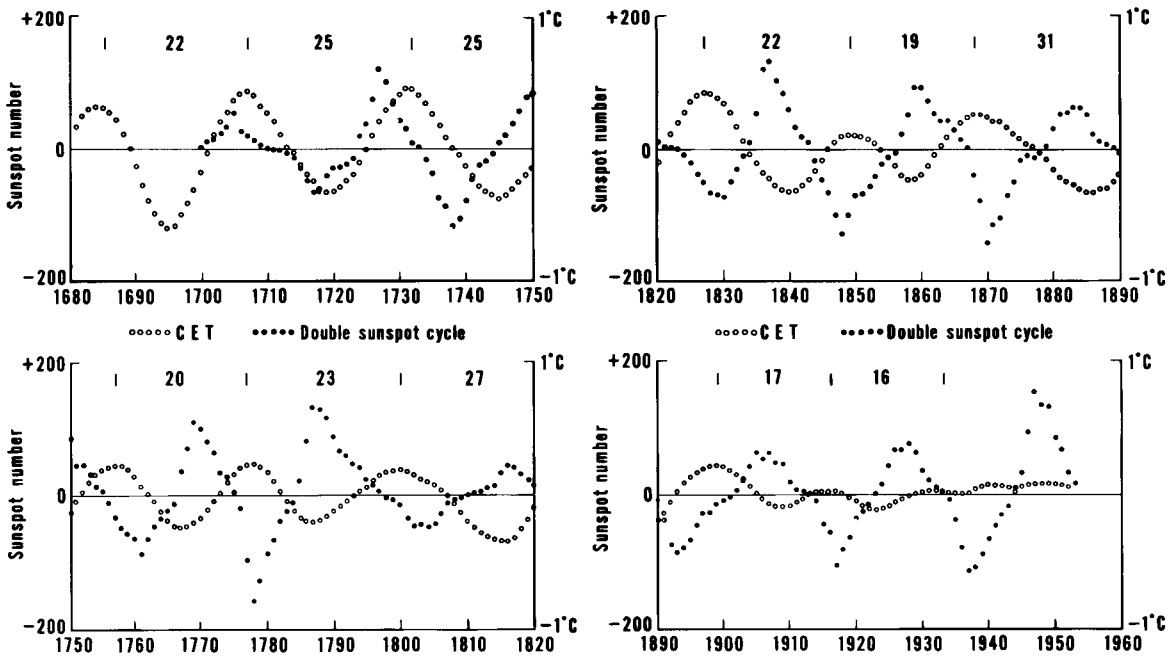


Figure 15. The '23-year' wavelength band-pass filtered series of annual mean Central England Temperature and the 'Hale' or double-sunspot cycle.

model and some of the problems concerning the mutual interaction of the spatial and time-scales of climatic 'events' which have to be considered for practical purposes. (See section 4 for an initial discussion). The pronounced geographical variation in the behaviour of rainfall may be reduced by expressing rainfall observed on a given time-scale as a percentage of its average value on that time-scale. For example, one month 'point', 'any rain-gauge' EW rainfall, has a markedly different frequency distribution from a series representing EW as a whole. Very rare dry events are drier at any point than events of equal rarity over EW as a whole while very wet events are wetter. This effect is less pronounced for events measured over longer time intervals and more pronounced over shorter time intervals. This difference of behaviour with varying time-scale reflects variations of the spatial correlation of rainfall; one-month rainfall is less well correlated at a given distance (it is more variable) than is 12-month rainfall, but it is better correlated than daily rainfall. The fact that point rainfall anywhere in EW having a 20-year return period tends to have a similar percentage of average value (the y-axis in Fig. 17) as 100-year rainfall over EW as a whole suggests that locally very dry areas will almost always be accompanied by much wetter areas elsewhere in EW. Thus the ability during droughts to transfer water over considerable distances within the area of EW could be valuable. The ratio of point to areal rainfall for a specified return period is often called the areal reduction factor, but better perhaps the areal adjustment factor (Folland, Kelway and Warrilow 1981).

8.2 Very heavy short duration rainfall

Fig. 18 shows a typical example of the shape of the frequency distributions for very heavy rainfall for several short durations, taken from the extensive work of Jenkinson (1975). This type of information is

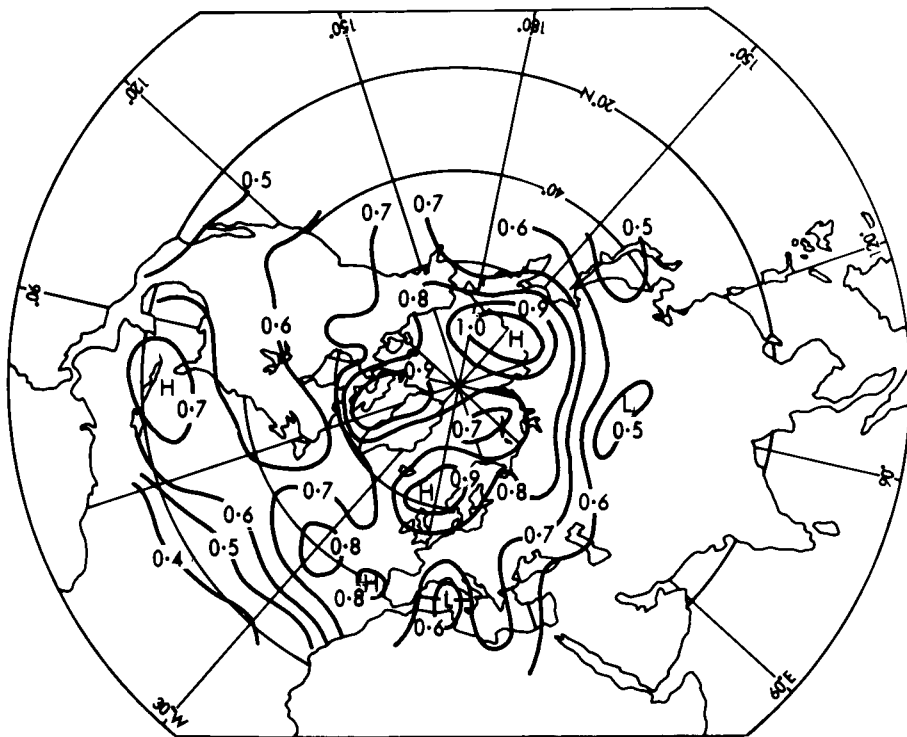


Figure 16. Ratio of root-mean-square amplitude of approximately 20-day to 60-day 500 mb geopotential fluctuations to root-mean-square amplitude on time-scales less than about 20 days; 1961-63.

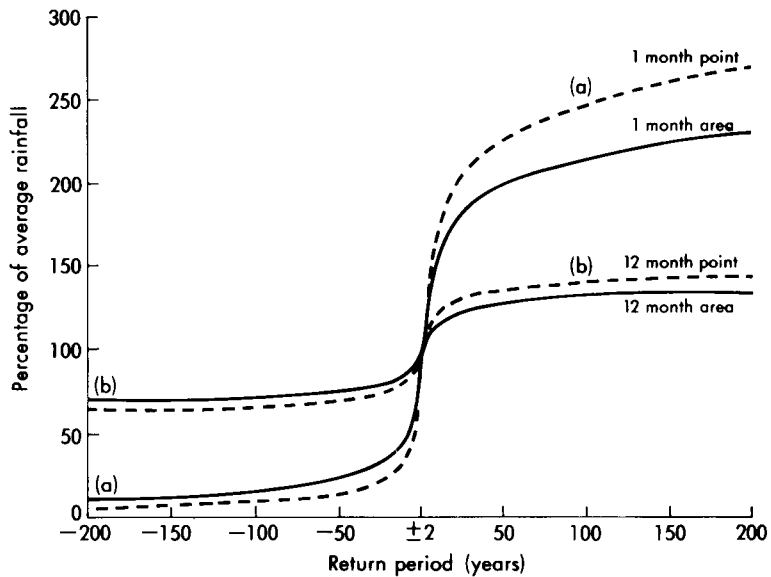


Figure 17. Percentage of average rainfall corresponding to various return periods for durations of 1 month and 12 months. Point curve for typical point in England and Wales; areal curve for England and Wales as a whole. Negative return periods represent deficiencies and positive return periods represent excesses. ± 2 represents a 50% chance of a wetter or a drier year.

used in dam, river flood protection, see *Flood Studies Report Volume I* (Natural Environment Research Council 1975) and sewer design for shortest durations, (see for example National Water Council 1981).

As can be seen from Fig. 18, short duration rainfall does not appear to converge to a maximum value as the return period becomes extremely large as might be expected on physical grounds. Most other variables for which long enough records are available do tend to converge toward a maximum, for example maximum daily temperature, whose value depends on the locality. Estimates of maximum possible rainfall are crucial in modern dam design where safety is the overriding factor; maxima are in fact estimated through the use of very simplified physical models. These difficulties of estimating statistically extreme rainfall have recently received attention (Warrilow in published discussion of the paper by Folland, Kelway and Warrilow (1981), same volume). It seems now that a key problem in the statistical calculations lies in a systematic change with return period in the average speed of movement of the rarer (convective) storms that contribute to the right-hand side of the curves in Fig. 18. Short duration heavy rain storms generally last considerably longer in the moving frame of reference of the rain storm than at an observing station rain-gauge, but it is likely that the heaviest rainfall totals measured by rain-gauges tend to result from the most slow-moving storms. A marked correlation between the speed of short-duration storms and measured rainfall is likely to violate seriously the assumptions underlying the extreme value analysis algorithms usually applied to short-duration heavy rainfalls. This aspect of the statistical interpretation of extreme climate data may be pertinent to the analysis of other meteorological phenomena.

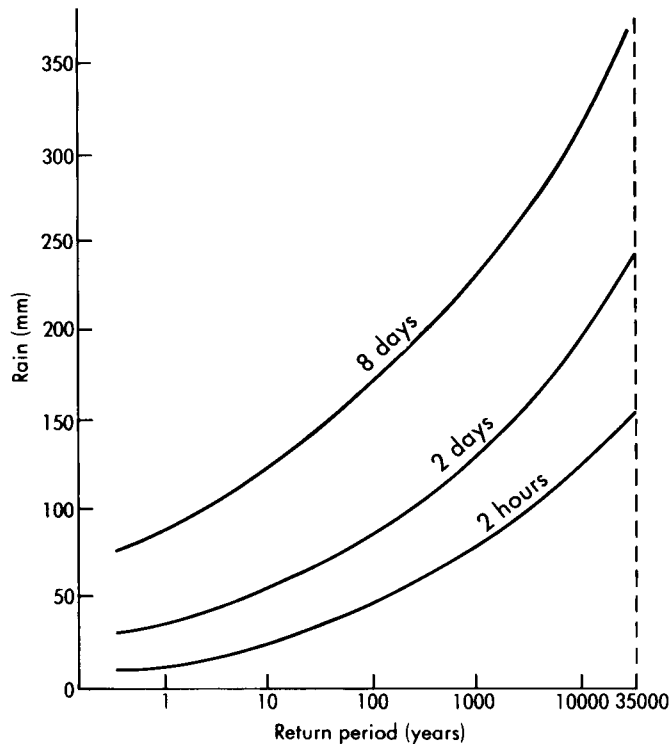


Figure 18. Typical relationship between rainfall total and return period at a point (south-east England).

8.3 An agricultural application

A contrasting application of climatic frequency data is shown in Fig. 19. Maize, a tropical grass, provides a very good source of winter cattle feed ('silage') but the climate of England and Wales is marginal to its success. Fig. 19 shows the percentage of years that a particular, very economic, form of silage can be successfully made from maize. In areas where more than two bad years in ten are likely to occur it may often not be economic to grow maize.

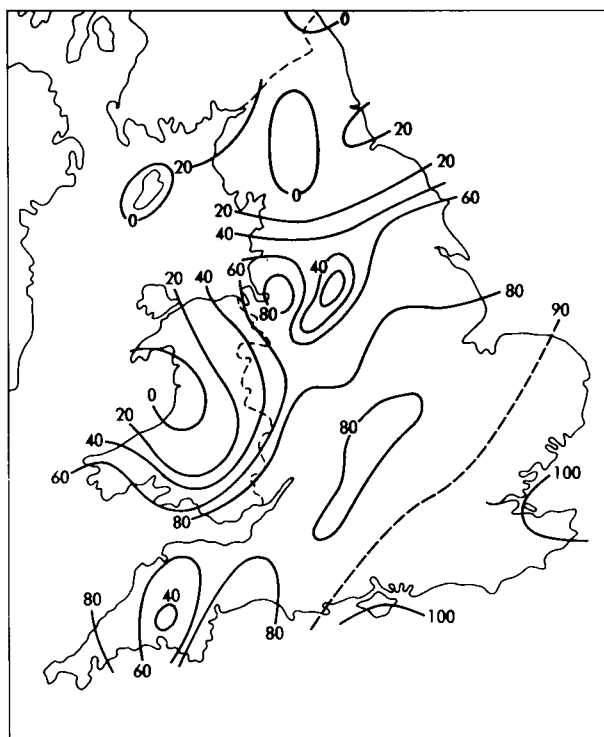


Figure 19. Percentage of years suitable for making Tower Silage from maize in England, Wales and the Isle of Man.(From Hough 1978.)

9. Conclusions

Prospects may soon improve for developing concepts about regional short-period climatic variability. Besides the greatly improved capability for integrating numerical atmospheric models, diagnostic data which allow daily atmospheric budgets of heat, moisture, momentum and radiation to be continuously monitored are becoming routinely available. The task is very challenging; long-range forecasting especially may depend for its development on some success in this field. The following words written a long time ago perhaps still apply:

Our knowledge of the properties of the atmosphere would therefore become of the highest utility to mankind, could the varieties of season, or recurrence of sudden changes of weather, be readily prognosticated. But this investigation is so intimately connected with circumstances which influence different climates, that a general table of prognostics can only be completed by the united labours and experience of the learned in every country.

Robertson (1808)

References

- Bader, M. J. and Warrilow, D. 1979 Why it was dry in the Autumn of '78. *Water, J Natl Water Council*, **25**, March 1979 2-5.
- Blackmon, M. L., Madden, R. A., Wallace, J. M. and Gutzler, D. S. 1979 Geographical variations in the vertical structure of geopotential height fluctuations. *J Atmos Sci*, **36**, 2450-2466.
- Craddock, J. M. 1964 Long-range weather forecasting in Great Britain. *Meteorol Mag*, **93**, 98-106.
- Folland, C. K. 1978 Scientific aspects of the 1975-6 drought in England and Wales. (Report on a meeting at the Royal Society, London, October 1977). *Hydrol Sci Bull*, 302-304.
- Folland, C. K., Kelway, P. S. and Warrilow D. A. 1981 The application of meteorological information to flood design. Inst Civ Eng, Flood Studies Rep. — Five Years On, 33-47.
- Gray, Barbara M. 1976 Medium term fluctuations of rainfall in southeastern England. *Q J R Meteorol Soc*, **102**, 627-638.
- Hastenrath, S. and Kaczmarczyk, E. B. 1981 On spectra and coherence of tropical climate anomalies. *Tellus*, **33**, 453-462.
- Haurwitz, M. W. and Brier, G. W. 1981 A critique of the superposed epoch analysis method: its application to solar-weather relations. *Mon Weather Rev*, **109**, 2074-2079.
- Hough, M. N. 1978 Mapping areas of Britain suitable for maize on the basis of Ontario Units. *ADAS Q Rev*, **31**, Winter 1978, 217-227.
- Jenkinson, A. F. 1975 Co-author of Flood Studies Report Vol II, NERC 1975.
- Korevaar, C. G. 1982 A comparative study of classifications of monthly mean sea surface temperature anomalies in the North Atlantic Ocean. *Meteorol Mag*, **111**, 14-18.
- Lamb, H. H. 1972 Climate: Present, Past and Future-Vol I. Fundamentals and Climate Now. Methuen.
- Manley, G. 1974 Central England Temperatures: monthly means 1659 to 1973. *Q J R Meteorol Soc*, **100**, 389-405.
- Mason, B. J. 1976 Towards the understanding and prediction of climatic variations. *Q J R Meteorol Soc*, **102**, 473-498.
- Miles, M. K. 1977 Atmospheric circulation during the severe drought of 1975/76. *Meteorol Mag*, **106**, 154-164.
- Murray, R. 1966 A note on the large-scale features of the 1962/3 winter. *Meteorol Mag*, **95**, 339-348.
- 1977 The 1975/6 drought over the United Kingdom — hydro-meteorological aspects. *Meteorol Mag*, **106**, 129-145.
- Namias, J. 1963 Large-scale air-sea interactions over the North Pacific from summer 1962 through the subsequent winter. *J Geophys Res*, **68**, 6171-6186.
- National Water Council 1981 Design and analysis of urban storm drainage — the Wallingford Procedure Vol. 1. Principles, methods and practice. Working party on the hydraulic design of storm sewers. D.o.E/NWC Standing Technical Committee Reports No. 28.
- Natural Environment Research Council 1975 Flood Studies Report Vol. I. London.
- Nicholls, N. 1980 Long-range weather forecasting: value, status and prospects. *Rev Geophys Space Phys*, **18**, 771-788.
- Painting, D. J. 1976 A study of some aspects of the climate of the Northern Hemisphere in recent years. *Sci Pap, Meteorol Off*, No. 35.
- Parker, D. E. 1982 Large-scale interannual variability of climate. *Meteorol Mag*, **111**, 193-208.
- Rasmusson, E. M. and Carpenter, T. H. 1982 Variations in tropical sea surface temperature and surface wind fields associated with the Southern Oscillation/El Nino. *Mon Weather Rev*, **110**, 354-384.
- Ratcliffe, R. A. S. 1977 A synoptic climatologists's viewpoint of the 1975/6 drought. *Meteorol Mag*, **106**, 145-154.
- Ratcliffe, R. A. S. and Murray, R. 1976 New lag associations between North Atlantic sea temperature and European pressure applied to long-range weather forecasting. *Q J R Meteorol Soc*, **96**, 226-246.

- Ratcliffe, R. A. S. and
Morris, R. M.
Rodriguez-Iturbe, I. and
Mejia, J. M.
Robertson, H.
- Rowntree, P. R.
- Sawyer, J. S.
- Schönwiese, C-D.
- Tabony, R. C.
- Wright, P. B.
- 1976 Under the weather. *Nat*, **264**, 4-5.
- 1974 On the transformation of point rainfall to areal rainfall. *Water Resour Res*, **10**, 729-735.
- 1808 A general view of the Natural History of the atmosphere, and its connections with the sciences of Medicine and Agriculture. Vol I Laing, Constable & Co and Deas, Edinburgh; and Cadell and Davies, and Longman, Hurst, Rees and Orme, London.
- 1972 The influence of tropical east Pacific Ocean temperatures on the atmosphere. *Q J R Meteorol Soc*, **98**, 290-321.
- 1976(a) Tropical forcing of atmospheric motions in a numerical model. *Q J R Meteorol Soc*, **102**, 583-605.
- 1976(b) Response of the atmosphere to a tropical Atlantic ocean temperature anomaly. *Q J R Meteorol Soc*, **102**, 607-625.
- 1965 Notes on the possible physical causes of long-term weather anomalies. WMO Tech Note 66, Geneva, 227-248.
- 1970 Observational characteristics of atmospheric fluctuations with a time scale of a month. *Q J R Meteorol Soc*, **96**, 610-625.
- 1979 Correlations and phases of band-pass filtered European air temperature series. *Beitr Phys Atmos*, **52**, 136-146.
- 1977 The variability of long-duration rainfall over Great Britain. *Sci Pap. Meteorol Off*, No. 37.
- 1975 Four mild winters — in Europe. *Weather*, **30**, 125-126.

Documentation of a Southern Oscillation index

By D. E. Parker

(Meteorological Office, Bracknell)

Summary

Monthly and seasonal values of the difference of mean-sea-level pressure between Tahiti (18 °S, 150 °W) and Darwin (12 °S, 131°E) are presented for the period from January 1935 to March 1983. A slight adjustment has been incorporated in order to take account of a change of observing time at Darwin. Extreme values of the pressure difference occurred from June 1982 onwards in association with anomalous behaviour of other elements of the Southern Oscillation.

1. Introduction

This paper attempts to satisfy the need for a tabulation of a Southern Oscillation index that is simple enough to be updated readily by any user. The mean-sea-level pressure-field index given by Wright (1977), although reliable, is not easily updated because it is based on principal component analysis. Similarly, areally-measured sea surface temperatures (Rasmusson and Carpenter 1982) and winds (Wyrтки 1980) are not simple to update and may also be analysis-dependent in data-sparse areas. Rainfall at Pacific islands may include local topographically forced components. The requirement for a simple but reliable index appears to be met best by the index recommended by Chen (1982) for diagnostic studies: Tahiti minus Darwin mean-sea-level pressure. The index is available throughout the period during which the Southern Oscillation can be studied most comprehensively, i.e. the period since the commencement of upper-air data, but for events before the opening of the Tahiti station in 1935, another index, such as Wright's (1977), must be used.

2. Tabulation and quality control of the monthly index

Monthly values of the difference in mean-sea-level pressure, Tahiti minus Darwin, are given in Table I for 1935 (the earliest year for which Tahiti data are available) to 1983 (March).

The sources of data were a magnetic tape from the USA National Climate Center, Asheville, NC up to December 1976, and CLIMAT monthly messages received at Bracknell over the Global Telecommunication System thereafter. CLIMAT messages were also used to fill in for the following data missing from the magnetic tape:

Tahiti: August and December 1961, and December 1974

Darwin: November 1961.

Australian annals were used to supply the following missing data:

Darwin: March, October and November 1973.

Two other values were missing: Darwin December 1974 and December 1976. The latter was filled by assuming a deviation from normal consistent with surrounding stations plotted on a routine monthly chart of mean-sea-level pressure anomalies. The former could not be filled in this way because the data for the entire Northern Territory of Australia were missing, probably as a result of the dislocation to communications caused by the tropical cyclone that struck Darwin in late December 1974. Therefore the value taken was the December normal plus the average of the deviation from normal of November 1974 and January 1975; the reliability of this procedure is open to question in view of the unusual nature of December 1974 with its tropical cyclone, but the seasonal mean (December to February) will be less seriously affected.

The tape values from 1955 to 1976 were compared with CLIMAT data as a cross-check; for earlier years, CLIMAT values were not available. The tape value for Tahiti for February 1965 was replaced by the CLIMAT value which agreed with the value in a national annal. Tape values for Darwin for October 1961, May 1972 and August 1972 were also replaced by CLIMAT values. The CLIMAT mean-sea-level values for Darwin for May and August 1972 appeared to be the correct ones in view of station-level pressures on the Asheville tape. The tape value for Darwin for October 1961 was climatologically unreasonable (6 mb below normal with no other values in 1882–1976 more than 3 mb below normal).

3. Adjustment for observing time

Up to 31 March 1939 the Darwin data were derived from $\frac{1}{2}$ (0017 + 0617 GMT) and thereafter from $\frac{1}{2}$ (2300 + 0500 GMT), (Smithsonian Institution 1947). An inhomogeneity will have resulted from the diurnal pressure cycle, but not from the semi-diurnal pressure cycle, because the data times remained six hours apart. The effect was estimated from data and graphs for many stations (not including Darwin) and regions, presented by Hofmeyr (1958). The necessary correction, based on a diurnal cycle amplitude of 0.85 mb with a maximum at 5 a.m. local time, was made by subtracting 0.2 mb from the Tahiti-minus-Darwin index for all months up to March 1939 inclusive. Table I includes this correction.

4. Seasonal index

The seasonal index in Table II is based on the values in Table I with northern winter being December to February and so on. The reader can use the means and standard deviations provided to create a normalized index. The skewness and kurtosis coefficients do not indicate any departure from a Gaussian distribution (Brooks and Carruthers 1953).

5. Behaviour of the index in 1982

During 1982 the Southern Oscillation entered the 'negative' phase with below normal mean-sea-level pressure at Tahiti, and above normal at Darwin. The lowest seasonal values of the series for northern summer, autumn and winter occurred in 1982–83 as did the lowest monthly values for August, September, November, and January to March, and the equal lowest monthly values for June and October. However, the associated episode of warmth in the equatorial Pacific Ocean has differed in major respects in timing and sequence from earlier events (US Climate Analysis Center, Diagnostics Branch, Special Climate Diagnostics Bulletin, 10 November 1982). In particular, the positive sea surface temperature anomalies developed during the southern winter rather than the southern summer which has usually been the season for this process. Also the anomalies were not preceded by equally large anomalies near the Ecuador–Peru coast. In addition it appears from preliminary upper-air data that the warming of the tropical troposphere normally associated with warm episodes of the equatorial Pacific Ocean (Hastenrath and Wu 1982) did not occur in 1982. This may be a consequence of an increase in global albedo as a result of the eruptions of El Chichon in Mexico in March and April 1982. The matter will be investigated and will be reported elsewhere.

Table II. Seasonal values of the difference of mean-sea-level pressure between Tahiti (18°S, 150°W) and Darwin (12°S, 131°E)

	1935	1936	1937	1938	1939	1940	1941	1942	1943	1944	1945	1946	1947	1948	1949	1950	1951
Northern winter (Dec. Jan. Feb.)		3.6	4.3	5.2	6.6	3.3	0.5	2.4	6.5	3.3	5.2	4.7	3.2	4.1	3.4	6.2	7.0
Northern spring (Mar. Apr. May)	3.0	3.7	2.9	2.9	3.6	1.0	1.3	2.3	3.6	2.7	3.2	1.7	2.6	2.7	2.8	4.7	1.5
Northern summer (June July Aug.)	1.1	0.8	1.1	3.4	1.6	-1.3	-1.4	1.8	1.5	0.8	2.4	0.1	2.2	0.9	0.5	4.1	0.2
Northern autumn (Sept. Oct. Nov.)	3.5	2.0	2.3	3.7	1.0	0.3	0.7	3.5	3.7	2.1	3.2	1.1	3.7	2.9	2.8	4.7	1.0
	1952	1953	1954	1955	1956	1957	1958	1959	1960	1961	1962	1963	1964	1965	1966	1967	1968
Northern winter (Dec. Jan. Feb.)	2.6	3.1	4.0	5.7	6.4	5.0	2.4	2.2	4.7	4.9	6.5	4.4	3.1	3.9	3.2	5.9	4.8
Northern spring (Mar. Apr. May)	2.8	1.1	3.0	3.1	4.4	2.0	2.2	3.6	3.6	1.7	2.3	3.4	3.9	2.4	1.2	2.9	3.0
Northern summer (June July Aug.)	1.7	0.2	1.9	3.6	3.0	0.8	1.9	0.6	1.8	1.1	1.1	0.5	2.6	-0.9	1.5	1.9	2.1
Northern autumn (Sept. Oct. Nov.)	2.8	1.8	3.1	5.2	3.9	1.6	2.3	3.6	3.5	2.9	3.8	1.1	4.4	0.5	2.5	2.8	2.3
	1969	1970	1971	1972	1973	1974	1975	1976	1977	1978	1979	1980	1981	1982	1983		
Northern winter (Dec. Jan. Feb.)	2.9	2.9	6.6	5.1	2.2	7.9	4.1	7.1	4.3	1.5	4.3	4.0	4.1	5.2	-1.7		
Northern spring (Mar. Apr. May)	2.0	2.7	5.1	1.9	2.7	4.8	4.2	3.6	1.2	2.7	2.4	1.5	1.8	2.3			
Northern summer (June July Aug.)	0.7	1.6	2.2	-0.5	2.7	2.3	4.1	0.0	-0.9	1.9	0.8	1.1	2.6	-1.7			
Northern autumn (Sept. Oct. Nov.)	1.5	5.0	4.9	1.1	5.6	3.8	5.6	2.7	0.8	2.4	2.4	2.2	2.9	-1.1			
1941-70	Mean	Standard deviation	Skewness	Kurtosis													
Northern winter (Dec. Jan. Feb.)	4.2	1.5	-0.08	-0.60													
Northern spring (Mar. Apr. May)	2.7	0.9	-0.11	-0.45													
Northern summer (June July Aug.)	1.4	1.2	-0.09	0.29													
Northern autumn (Sept. Oct. Nov.)	2.8	1.2	-0.03	-0.75													

References

- Brooks, C. E. P. and Carruthers, N. 1953 Handbook of statistical methods in meteorology. London. HMSO.
- Chen, W. Y. 1982 Assessment of Southern Oscillation sea-level pressure indices. *Mon Weather Rev*, **110**, 800–807.
- Hastenrath, S. and Wu, W. L. 1982 Oscillations of upper-air circulation and anomalies in the surface climate of the tropics. *Arch Meteorol Geophys Bioklimatol*, **31**, 1–37.
- Hofmeyr, W. L. 1958 Diurnal and semi-diurnal oscillations of surface pressure in tropical regions. Pretoria, Weather Bureau, Southern Hemisphere, *Atmos Proj Notas*, **7**, 6–20.
- Rasmusson, E. H. and Carpenter, T. H. 1982 Variations in tropical sea surface temperature and surface wind fields associated with the Southern Oscillation/El Niño. *Mon Weather Rev*, **110**, 354–384.
- Smithsonian Institution 1947 World weather records 1931–1940. Washington D. C.
- Wright, P. B. 1977 The Southern Oscillation — patterns and mechanisms of the teleconnections and the persistence. University of Hawaii, Hawaii Institute of Geophysics OCE-76-23173.
- Wyrтки, K. 1980 Comparison of four equatorial wind indices in the Pacific and El Niño outlook for 1981. Washington D.C., US Department of Commerce, Proceedings of the Fifth Annual Climate Diagnostics Workshop, 211–218.

THE METEOROLOGICAL MAGAZINE

No. 1331

June 1983

Vol. 112

CONTENTS

	<i>Page</i>
Radar and rain-gauge observations of a severe thunderstorm near Manchester: 5/6 August 1981. M. J. Bader, C. G. Collier and F. F. Hill	149
Regional-scale interannual variability of climate — a north-west European perspective. C. K. Folland	163
Documentation of a Southern Oscillation index. D. E. Parker	184

NOTICES

It is requested that all books for review and communications for the Editor be addressed to the Director-General, Meteorological Office, London Road, Bracknell RG12 2SZ and marked 'For Meteorological Magazine'.

The responsibility for facts and opinions expressed in the signed articles and letters published in this magazine rests with their respective authors.

Applications for postal subscriptions should be made to HMSO, PO Box 276, London SW8 5DT.

Complete volumes of 'Meteorological Magazine' beginning with Volume 54 are now available in microfilm form from University Microfilms International, 18 Bedford Row, London WC1R 4EJ, England.

Full-size reprints of out-of-print issues are obtainable from Johnson Reprint Co. Ltd. 24-28 Oval Road, London NW1 7DX, England.

Please write to Kraus microfiche, Rte 100, Millwood, NY 10546, USA, for information concerning microfiche issues.

© Crown copyright 1983

Printed in England by Robendene Ltd., Amersham, Bucks.
and published by
HER MAJESTY'S STATIONERY OFFICE

£2 monthly
Dd. 736047 K15 6/83

Annual subscription £26.50 including postage
ISBN 0 11 726935 2
ISSN 0026-1149